



Author(s)	Slotboom, David R.
Title	Kinematics of atomic charge transfer collisions.
Publisher	Monterey, California: U.S. Naval Postgraduate School
Issue Date	1963
URL	<a href="http://hdl.handle.net/10945/12524">http://hdl.handle.net/10945/12524</a>

This document was downloaded on May 12, 2015 at 03:36:06



<http://www.nps.edu/library>

Calhoun is a project of the Dudley Knox Library at NPS, furthering the precepts and goals of open government and government transparency. All information contained herein has been approved for release by the NPS Public Affairs Officer.

**Dudley Knox Library / Naval Postgraduate School  
411 Dyer Road / 1 University Circle  
Monterey, California USA 93943**



<http://www.nps.edu/>

NPS ARCHIVE  
1963  
SLOTBOOM, D.

KINEMATICS OF ATOMIC  
CHARGE-TRANSFER COLLISIONS  
DAVID R. SLOTBOOM

KINEMATICS OF ATOMIC  
CHARGE-TRANSFER COLLISIONS

\* \* \* \* \*

David R. Slotboom

KINEMATICS OF ATOMIC  
CHARGE-TRANSFER COLLISIONS

by

David R. Slotboom  
(1)  
Lieutenant, United States Navy

Submitted in partial fulfillment of  
the requirements for the degree of

MASTER OF SCIENCE  
IN  
PHYSICS

United States Naval Postgraduate School  
Monterey, California

1 9 6 3

KINEMATICS OF ATOMIC  
CHARGE-TRANSFER COLLISIONS

by

David R. Slotboom

This work is accepted as fulfilling  
the thesis requirements for the degree of

MASTER OF SCIENCE

IN

PHYSICS

from the

United States Naval Postgraduate School

## ABSTRACT

The relationship between the angles of emission and the energy of the slow secondary ion emitted in the reaction  $A^+ + B \rightarrow A + B^+ + \Delta E$  is calculated for a number of collisions between various inert gases, hydrogen, nitrogen, and oxygen. The calculations are carried out for several incident ion energies and for many of the excited states of the incident and resulting system which appear experimentally resolvable. Two types of targets are considered: (a) a stationary gas, (b) a gas curtain with a Maxwellian speed distribution. Machine calculations were performed for 25 reactions, several incident ion energies (including isotope effects) and several excited states in each case.

The writer wishes to express his appreciation for the assistance and encouragement given him by Professor Otto Heinz of the U. S. Naval Postgraduate School and Doctors Don C. Lorents and James R. Peterson of Stanford Research Institute.

# TABLE OF CONTENTS

Section	Title	Page
1.	Introduction	1
2.	Collision Kinematics for Stationary Target Atoms	5
2.1	Inert Gases	14
2.2	Hydrogen, Nitrogen, and Oxygen	26
3.	Nonstationary Target Atoms	30
4.	Bibliography	36
5.	Appendices	
A.	Computed values of the energy defect for charge transfer reactions of inert gases	37
B.	Computed values of the energy defect for charge transfer reactions of hydrogen, nitrogen, and oxygen	46
C.	Curves relating the angle of emission of the secondary ion to its energy for reactions of inert gases	57
D.	Curves relating the angle of emission of the secondary ion to its energy for reactions of hydrogen, nitrogen, and oxygen	73
E.	The angular distribution of secondary ions of a fixed energy due to the distribution of speeds of the initial atom	82

# LIST OF ILLUSTRATIONS

Figure		Page
1.	Collision process when the initial atoms are stationary	5
2.	Possible roots for the energy of the secondary ions	8
3.	Relationship of parameters in the center of mass system to the laboratory system after collision	9
4.	Transformation of velocities when the energy defect equals $-mE_1/M_3$	11
5.	Transformation of velocities when the energy defect is greater than $-mE_1/M_3$	12
6.	Transformation of velocities when the energy defect is less than $-mE_1/M_3$	12
7.	Physically real roots for the energy of the secondary ions	13
8.	Collision process when the initial atoms have a Maxwellian speed distribution in the positive y direction	30



## 1. Introduction.

When two atomic systems collide with energies comparable to their electronic binding energies (a few ev to a few kev) a great variety of phenomena can occur. The quantum mechanical description of such collisions is in general very complex and only for the very simplest cases does an adequate theory exist. We are therefore forced to depend heavily on experimental information for our understanding of these collision processes.

If we consider the collision of a positive ion and a neutral atom in this energy region the following processes can occur:

elastic scattering

electronic excitation

transfer of electronic excitation

ionization

charge transfer (involving one or more electrons)

Almost all measurement of charge transfer cross sections carried out so far have measured total cross sections which represent a summation over all excited states and angles. The calculations presented here constitute the initial phase of a program which will attempt to measure the atomic charge transfer cross sections for specific final and initial states of the interacting systems. Such information should prove useful in the development of a detailed theory of the charge transfer process.

We shall restrict ourselves to the case in which a single electron is transferred. If a positive ion collides with a neutral, atom charge transfer may occur via one of the processes

- a)  $A^+ + B \longrightarrow A + B^+ + \Delta E$
- b)  $A^+ + B \longrightarrow A' + B^+ + \Delta E$
- c)  $A^+ + B \longrightarrow A + B^{+'} + \Delta E$
- d)  $A^+ + B \longrightarrow A' + B^{+'} + \Delta E$
- e)  $A^{+'} + B \longrightarrow A + B^+ + \Delta E$
- f)  $A^{+'} + B \longrightarrow A' + B^+ + \Delta E$
- g)  $A^{+'} + B \longrightarrow A + B^{+'} + \Delta E$
- h)  $A^{+'} + B \longrightarrow A' + B^{+'} + \Delta E$

where the prime indicates excited states. It is also possible that the initial atom may be in an excited state. However, if the initial atoms are those of a gas at room or oven temperatures this is unlikely, so this case is not considered.

The following definitions and notation will be used to describe the above reactions:

The ion  $A^+$  or  $A^{+'}$  is the primary ion.

The target gas atom (B) is the initial atom.

The atom (A or A') formed by the charge transfer is the final atom.

The ion ( $B^+$  or  $B^{+'}$ ) formed from the gas atom is the secondary ion.

$M_0$ ,  $E_0$ , and  $v_0$  are respectively the mass, energy, and speed of the initial atom.

$M_1$ ,  $E_1$ , and  $v_1$  are respectively the mass, energy, and speed of the primary ion.

$M_2$ ,  $E_2$ , and  $v_2$  are respectively the mass, energy, and speed of the secondary ion.

$M_3$ ,  $E_3$ , and  $v_3$  are respectively the mass, energy, and speed of the final atom.

$\Delta E$  is the energy defect defined as the difference in energy between the final atom and the primary ion minus the difference in energy between the initial atom and the secondary ion.

Reaction a will be called the ground state reaction.

Reaction b will be called the atom excitation reaction.

Reaction c will be called the ion excitation reaction.

Reaction e will be called the excited ion reaction.

The term reaction will refer to a general reaction or one of the reactions above when described with the proper adjectives.

The term transition will be used in a restricted sense to mean reactions between particles of specific initial and final energy states. Thus for a given transition  $\Delta E$  is unique and can be calculated.

For a charge transfer reaction between a particular primary ion and initial atom the possible transitions can be determined, from which the value of the energy defect for each transition can be calculated. The energy of the secondary ion can be determined as a function of the parameters  $M_1$ ,  $M_2$ ,  $M_3$ ,  $E_1$ ,  $\Delta E$ , and the angle  $\theta$  which is defined as the angle between the direction of the primary ion and the direction of the secondary ion. For a given transition  $M_1$ ,  $M_2$ ,  $M_3$ , and  $\Delta E$  are specified so  $E_2$  is a function of only  $E_1$  and  $\theta$ .  $E_1$  can be controlled experimentally so for a specified transition  $E_2$  is actually a function of  $\theta$  only. Thus by experimentally measuring the number of secondary ions which come out of the reaction at a particular angle  $\theta$  and which have corresponding energy  $E_2$ , as determined by the relationship between  $E_2$  and  $\theta$ , the differential charge transfer cross section for the particular transition can in principle be determined.

Our purpose here is: First to determine the dependence of  $E_2$  on  $\theta$  and the other known parameters. Second, to determine the possible transitions for each of a number of reactions, and from these compute the relationship between the angle of emission and the energy of the secondary ion for each transition. Then decide for which of these reactions it might be possible to distinguish the secondary ions emitted from different transitions, and hence, be able to measure the differential charge transfer cross section. Two groups of reactions will be considered; (a) reactions between the inert gases, and (b) reactions between atomic hydrogen, nitrogen, and oxygen. Third, as the above calculations will assume that the initial atoms are at rest, the dependence of  $E_2$  on  $\theta$  will finally be derived allowing that the initial atoms compose a gas curtain with a Maxwellian speed distribution. From this the relationship between the angles of emission and the energy of the secondary ion will be calculated giving the angular distribution of secondary ions of a constant energy.



## 2. Collision Kinematics for Stationary Target Atoms.

The system to be considered is shown schematically in figure 1 where it is assumed that the initial atom is at rest.

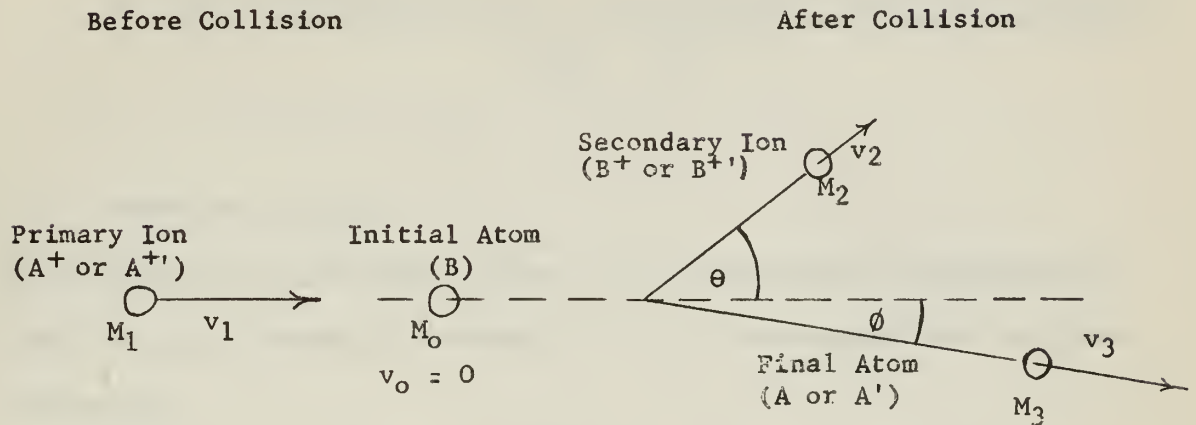


Figure 1.  
Collision process when the  
initial atoms are stationary

From conservation of non-relativistic energy

$$1) \quad \frac{1}{2} M_1 v_1^2 + \Delta E = \frac{1}{2} M_2 v_2^2 + \frac{1}{2} M_3 v_3^2$$

and conservation of momentum

$$2) \quad M_1 v_1 = M_2 v_2 \cos \theta + M_3 v_3 \cos \phi$$

$$3) \quad 0 = M_2 v_2 \sin \theta + M_3 v_3 \sin \phi$$

v<sub>3</sub> and ϕ can be eliminated resulting in

$$4) \quad (M_3 + M_2) E_2 - (M_3 - M_1) E_1 - M_3 \Delta E = 2(M_1 M_2 E_1 E_2)^{1/2} \cos \theta$$

or solving for E<sub>2</sub> explicitly

$$5) E_2 = \frac{2M_1M_2E_1\cos^2\theta + (M_3+M_2)[mE_1 + M_3\Delta E]}{(M_3 + M_2)^2}$$

$$+ \frac{2\cos\theta[M_1^2M_2^2E_1\cos^2\theta + M_1M_2E_1(M_3+M_2)(mE_1 + M_3\Delta E)]^{1/2}}{(M_3 + M_2)^2}$$

where  $m = M_3 - M_1$

It is seen that  $E_2$  is double valued. It is desirable to determine if both roots are physically meaningful or if an extraneous root has been introduced.

By squaring each of the two terms on the right side of equation 5 separately it is seen that the absolute value of the single valued term is always greater than or equal to the absolute value of the double valued term. Therefore, the sign of both roots of  $E_2$  is either the same as the sign of the single valued term, or  $E_2$  is equal to zero. It is also noted that the single valued term of equation 5 will be negative only when

$$\Delta E < - \left[ \frac{2M_1M_2E_1\cos^2\theta}{M_3(M_3+M_2)} + \frac{m}{M_3} \right]$$

but this also satisfies the condition

$$\Delta E < - \left[ \frac{M_1M_2E_1\cos^2\theta}{M_3(M_3+M_2)} + \frac{m}{M_3} \right]$$

that the square root term is negative, and hence  $E_2$  is imaginary. Therefore, all real roots of  $E_2$  are either positive or zero.

Three cases can be distinguished in considering  $E_2$  as a function of  $\theta$  for  $0 \leq \theta \leq \pi$ .

Case 1)

$$\Delta E = - \frac{mE_1}{M_3}$$

Then  $E_2$  becomes

$$E_2 = \frac{2M_1M_2E_1\cos^2\theta \pm 2M_1M_2E_1\cos^2\theta}{(M_3 + M_2)^2}$$

so that  $E_2$  has one positive and one zero root for all values of  $\theta$ . Experimentally the zero root is unimportant as it indicates the secondary ion is at rest.

Case 2)

$$\Delta E > - \frac{mE_1}{M_3}$$

The term under the radical will always be positive, so  $E_2$  will have two real positive roots for every value of  $\theta$ .

Case 3)

$$\Delta E < - \frac{mE_1}{M_3}$$

The term under the radical is negative for all values of  $\theta$  greater than some  $\theta_0$  but less than  $(\pi - \theta_0)$ . Therefore  $E_2$  will not have real roots in this region, but will have two real positive roots for all values of  $\theta$  less than  $\theta_0$  and all values of  $\theta$  greater than  $(\pi - \theta_0)$ .

The mathematically possible roots for each of these cases are summarized in figure 2.

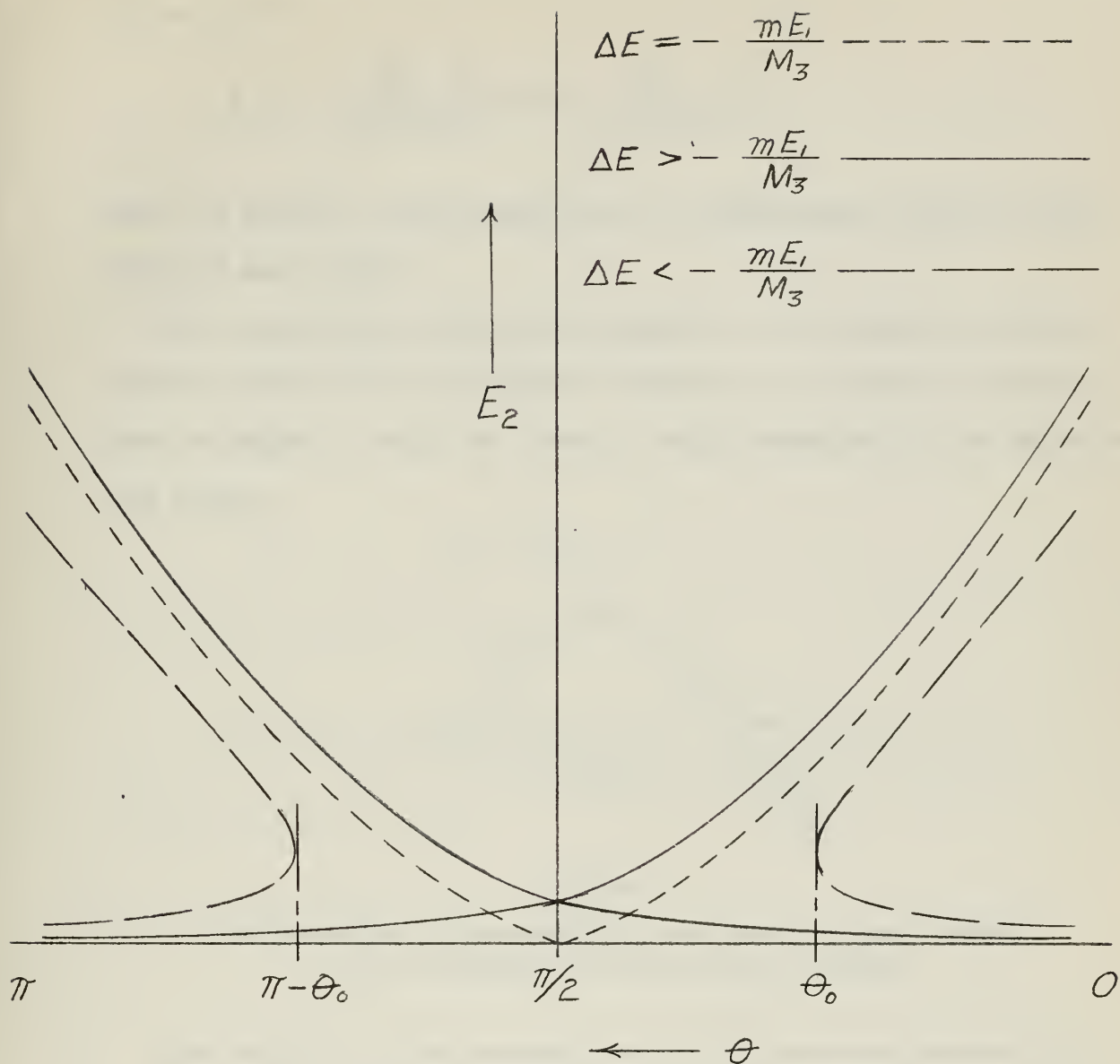


Figure 2.

Possible roots for the energy of the secondary ions

To determine which of these roots are physically meaningful the collision is examined in the center of mass coordinate system. The energy



of the secondary ion in the center of mass system ( $E_2'$ ) can be written as a function of the energy of the initial ion in the laboratory coordinate system ( $E_1$ ) by

$$6) \quad E_2' = \frac{M_3}{M_2 + M_3} \left[ \Delta E + \frac{M_0}{M_0 + M_1} E_1 \right]$$

Hence the energy of the secondary ions is independent of angle in the center of mass system.

The relationship between the parameters in the center of mass coordinate system and the laboratory coordinate system after collision is shown in figure 3, where the "primes" denote parameters in the center of mass system.

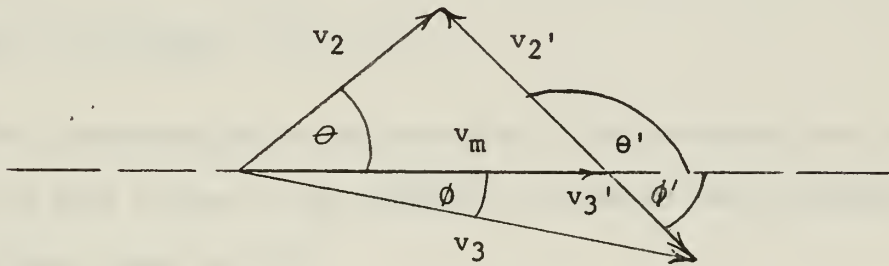


Figure 3.

Relationship of parameters in the center of mass system to the laboratory system after collision

The velocity of the secondary ion in the laboratory system ( $\vec{v}_2$ ) is the vector sum of its velocity in the center of mass system ( $\vec{v}_2'$ ) and the velocity of the center of mass in the laboratory systems ( $\vec{v}_m$ ). The speed of the secondary ion in the center of mass system ( $\vec{v}_2'$ ) is found from equation 6 to be,

$$7) \quad v_2' = \left[ \frac{2 M_3}{M_2 (M_2 + M_3)} \left( \Delta E + \frac{M_0}{M_0 + M_1} E_1 \right) \right]^{1/2}$$

and the speed of the center of mass is

$$8) \quad v_m = \frac{M_1}{M_0 + M_1} v_1 = \left[ \frac{2 M_1}{(M_0 + M_1)^2} E_1 \right]^{1/2}$$

For a specific transition and for a given  $E_1$  each of these speeds is a constant.

If  $\Delta E$  is set equal to  $-\frac{m E_1}{M_3}$  in equation 8 and making use of the relation

$$9) \quad M_0 + M_1 = M_2 + M_3$$

then  $v_2'$  becomes

$$10) \quad v_2' = \left[ \frac{2 M_1}{(M_0 + M_1)^2} E_1 \right]^{1/2}$$

so that, in this case  $v_2' = v_m$

The transformation of the velocity of the secondary ion from the center of mass system to the laboratory system is now considered for each of the three cases of  $\Delta E$ .

$$\text{Case 1)} \quad \Delta E = -\frac{m E_1}{M_3}$$

As shown above  $v_2' = v_m$ . The vector addition of the two vectors  $\vec{v}_m$  and  $\vec{v}_2'$  is shown in figure 4.  $\vec{v}_m$  is a vector in the direction of the initial particle,  $\vec{v}_2'$  can be any vector which is a radius of the circle, and the angle between the two vectors is  $\theta'$ . As  $\theta'$  goes from zero to  $\pi$ ,  $\theta$  goes from zero to  $\pi/2$ , and  $v_2$  and, hence,  $E_2$  goes from a maximum to a minimum of zero. In this case the solutions of equation 5 with  $\theta$  greater than  $\pi/2$  are extraneous.

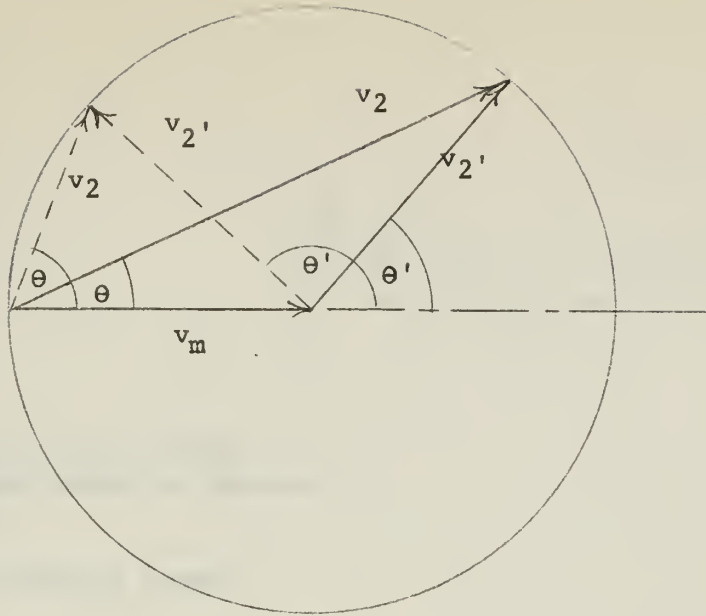


Figure 4.

Transformation of velocities when the energy defect equals  $-mE_1/M_3$ .  
(two vector additions shown)

Case 2)

$$\Delta E > - \frac{mE_1}{M_3}$$

From equations 7 and 10,  $v_2'$  will be greater than  $v_m$ . The vector addition is shown in figure 5.

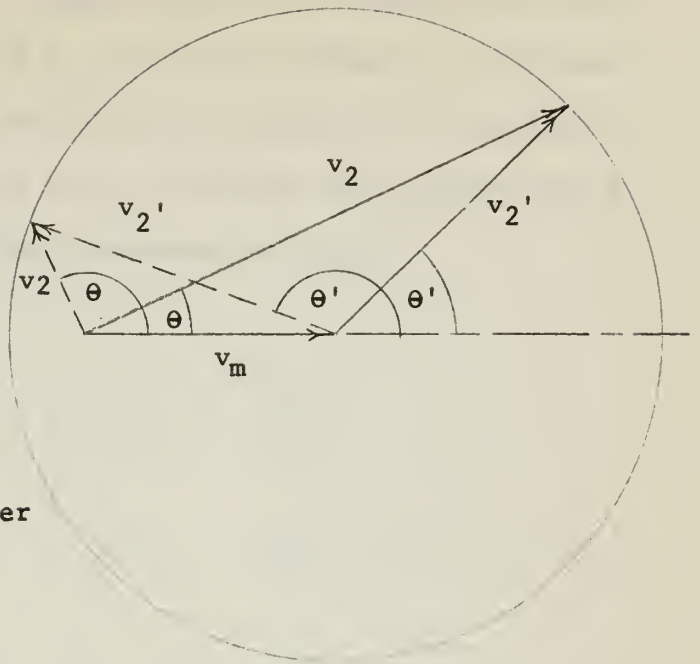


Figure 5.

Transformation of velocities  
when the energy defect is greater  
than  $-mE_1/M_3$ .

(Two vector additions shown)

Now as  $\theta'$  ranges zero to  $\pi$ ,  $\theta$  also ranges from zero to  $\pi$ , and  $v_2$  goes from a maximum to a minimum. Therefore  $E_2$  is a single valued function of  $\theta$  and has its maximum value when  $\theta$  is zero and its minimum value when  $\theta$  is  $\pi$ .

Case 3) 
$$\Delta E < -\frac{mE_1}{M_3}$$

From equations 7 and 10,  $v_2'$  is less than  $v_m$ . The vector addition is shown in figure 6.

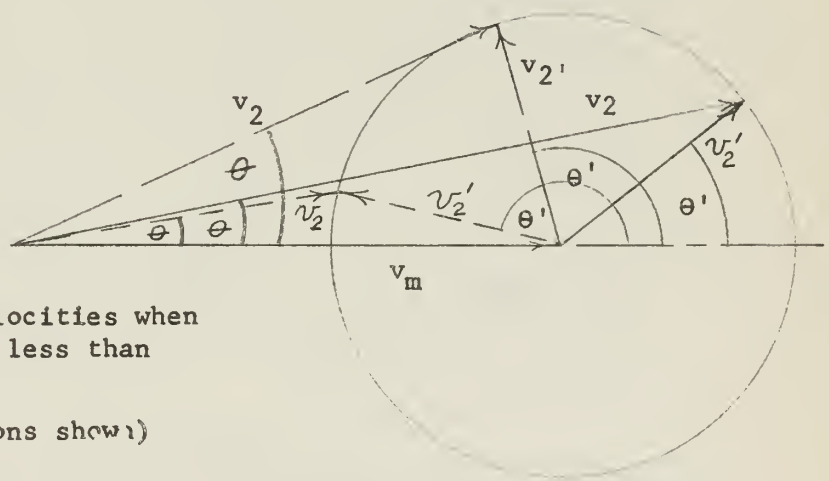


Figure 6.

Transformation of velocities when  
the energy defect is less than  
 $-mE_1/M_3$ .

(Three vector additions shown)

As  $\theta'$  ranges from zero to  $\pi$ ,  $\theta$  ranges from zero to some  $\theta_0$  less than  $\pi/2$ , and then back to zero, and  $v_2$  goes from a maximum to a minimum. Thus,  $E_2$  is a double valued function of  $\theta$  for values of  $\theta$  less than  $\theta_0$ , and has no physically meaningful roots for values of  $\theta$  greater than  $\theta_0$ .

The physically real roots are summarized in figure 7.

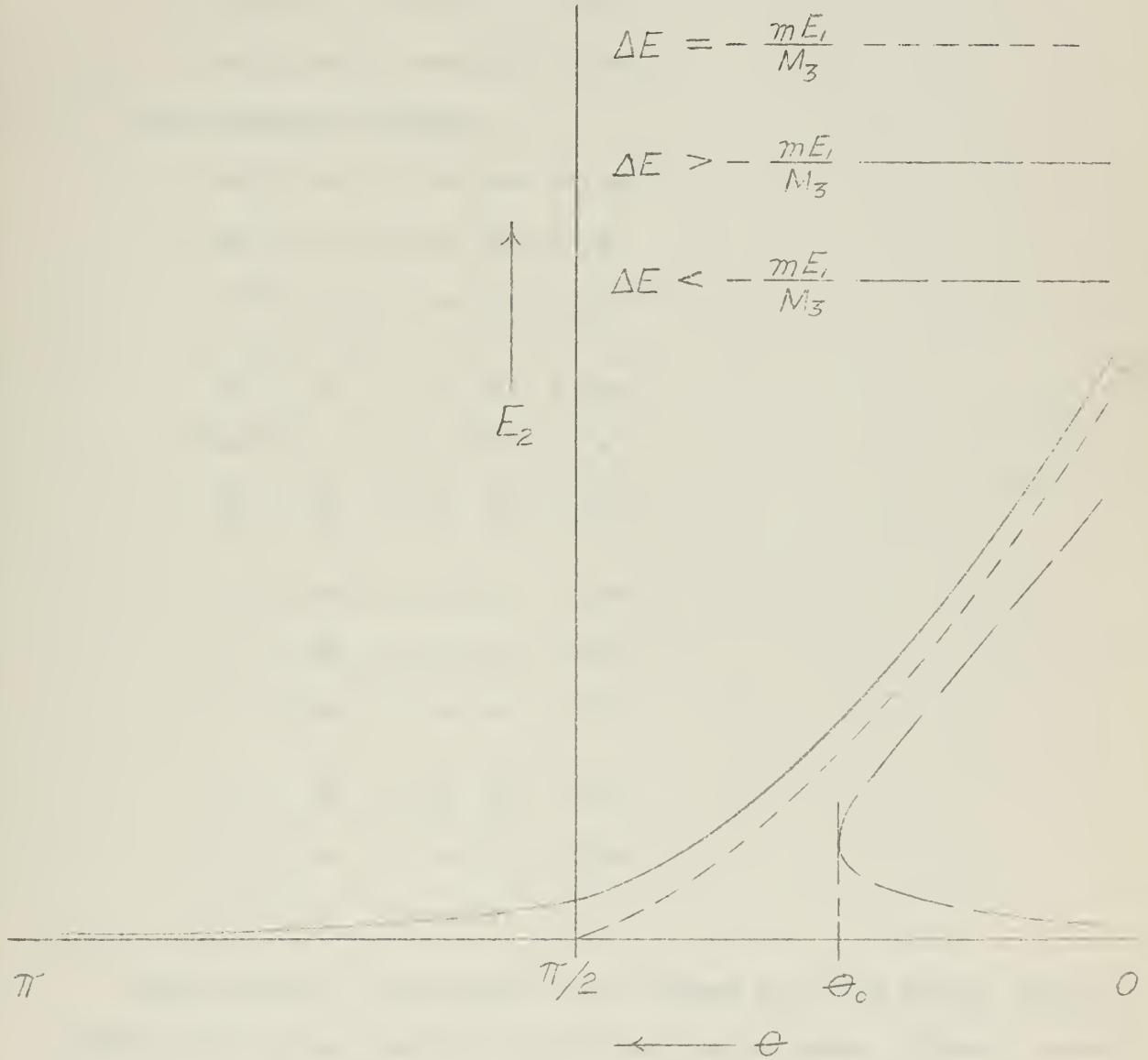


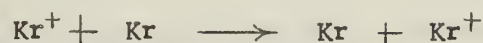
Figure 7.

Physically real roots for the energy of the secondary ions.

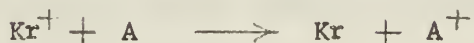
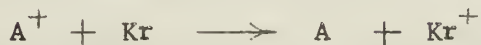
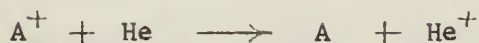
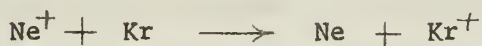
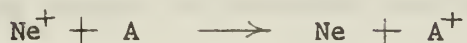
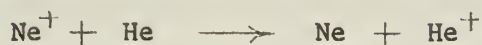
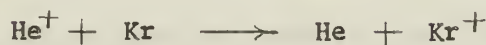
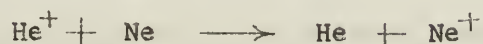
## 2.1 Inert Gases.

The possible transitions for each of the following reactions are now considered.

### Resonance reactions



### Non resonance reactions



Experimentally, the primary ion is formed in an ion source and then travels some distance before colliding with a gas atom. (Typical transit times are on the order of 10  $\mu$ sec.). Although the primary ion might very well be formed in an excited state, unless this is a metastable



state the ion will most likely decay to the ground state before collision with the initial atom occurs. Therefore, transitions in which the primary ion is in an excited state will be considered only if the primary ion is in a metastable state. Since none of the single ionized inert gases have metastable states,<sup>1</sup> none of these transitions are considered, and hence reactions e through h on page 2 are eliminated for the inert gases.

The energy defects were computed for the transitions which give rise to the lowest absolute values of the energy defect. These include the ground state reaction, the atom excitation reaction for the first few excited states of the final atom, and in some cases the ion excitation reaction for the first few excited states of the secondary ion. As the level of the excited state of the final atom or the secondary ion is increased the absolute value of the energy defect increases.

As  $\Delta E$  becomes increasingly negative the difference in the values of succeeding  $\Delta E$ 's decreases, giving rise to values of  $E_2$  which cannot be resolved experimentally. Therefore, reactions of higher absolute values of  $\Delta E$  are not considered. Reaction d is necessarily in this category since energy must be provided to excite both the final atom and ion which will give rise to a large negative  $\Delta E$ . Therefore, only the ground state reaction, the atom excitation reaction, and the ion excitation reaction are considered for inert gases.

The computed energy defects for each of the inert gas reactions are tabulated in appendix A.

Using these values of  $\Delta E$ ,  $E_2$  was calculated as a function  $\theta$  for each of the following values of  $E_1$ : 20 eV, 100 eV, 200 eV, 500 eV. The

<sup>1</sup>R. L. Kelly, Unpublished Grotrian Diagrams, U. S. Naval Postgraduate School

masses used were those of the most abundant isotope of each element. This is entirely satisfactory for helium and argon in which the most abundant isotope accounts for respectively 100.00% and 99.6% of the gas. However, only 90.92% of neon is  $\text{Ne}^{20}$  and only 56.9% of krypton is  $\text{Kr}^{84}$ .

For the two reactions involving both neon and krypton it was decided that the presence of the isotopes of both neon and krypton ( $\text{Ne}^{22}$ ,  $\text{Kr}^{82}$ , and  $\text{Kr}^{86}$  would have to be considered) would lead to too many possible transitions to make experimental resolution possible. Therefore, no further consideration was given to these two reactions. The other reactions involving krypton were considered, but, as will be seen below, even by neglecting the effect of the isotopes of krypton they cannot be resolved experimentally. Therefore effects of the isotopes of krypton were not considered.

Reactions involving neon are of experimental interest. Therefore, for the neon reactions, calculations of  $E_2$  as a function of  $\theta$  were also made using the mass of  $\text{Ne}^{22}$ , the second most abundant isotope of neon.  $\text{Ne}^{22}$  accounts for 8.82% of neon, so that together  $\text{Ne}^{20}$  and  $\text{Ne}^{22}$  make up 99.74% of the gas. The effect of this isotope of neon on the reactions is considered below.

A summary of the results of the calculations of equation 5 is now given. The effect of the value of the energy of the primary ion is considered first, and the following observations are made.

1. The difference in the values of  $E_2$  between two adjacent transitions is rather insensitive to  $E_1$ , at least over the range of  $E_1$  considered.

2. For a given transition the change of  $E_2$  with respect to  $\theta$  is dependent on  $E_1$ , the slope increasing with increasing values of  $E_1$ .



3. The maximum angle of emission of the secondary ion in a given endothermic transition decreases as the value of  $E_1$  decreases.

4. The difference, between two adjacent endothermic transitions, in the maximum angle of emission of the secondary ion increases as the value of  $E_1$  decreases.

Two criteria must be met to experimentally distinguish between two adjacent transitions. First, at a given  $\theta$  the values of the energy of the secondary ions must differ by a minimum of about two electron volts. Second, over a one degree increment of  $\theta$  about the given angle the values of the energy of the secondary ions should not overlap. From the above observations it is seen that the first criterion is not significantly affected by the value of  $E_1$ . However, the second criterion is; the greater the value of  $E_1$  the more likely it is that the values of  $E_2$  overlap. Therefore, decreasing the value of  $E_1$  increases the possibility of resolving adjacent transitions. However, there is a practical limit to the smallness of  $E_1$ . First, due to space charge effects, decreasing  $E_1$  decreases the beam intensity of the initial ions. Second, as  $E_1$  decreases the ratio  $a|\Delta E|/(h\nu_i)$  increases. Then according to the quasi-adiabatic analysis suggested by Massey /1/ (for inelastic collisions the cross section is small when  $a|\Delta E|/(h\nu_i) \gg 1$ ) the charge transfer cross section will become very small. Then as  $E_1$  is decreased it is expected that the number of particles undergoing a specific reaction will decrease sharply, making detection difficult.

This second concept is consistent with the findings of J. B. Hasted /2/ and N. V. Fedorenko /3/ which indicate that in a charge transfer reaction the great majority of the final atoms are emitted at very small

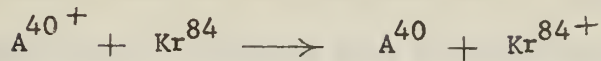
angles with the initial beam. Therefore, the secondary ions must make large angles with the initial beam. However, the above observations on the effect of changing  $E_1$  show that decreasing  $E_1$  decreases the maximum angle of emission of the secondary ions, so that for sufficiently small values of  $E_1$  no secondary ions are emitted at large angles. A logical conclusion, then, is that very few charge transfer collisions take place at these low values of  $E_1$ . Thus the minimum value of  $E_1$  to be considered can be stated in terms of the maximum angle which secondary ions in endothermic transitions are emitted. This maximum value of  $\theta$  was rather arbitrarily taken to be  $50^\circ$ .

Consider now the criterion that the energy of the secondary ions emitted from adjacent transitions must differ by a minimum of about two electron volts for the transitions to be resolved experimentally. It was found that for this criterion to possibly be met the values of  $\Delta E$  of the two transitions must differ by at least one electron volt. Since resolving between transitions of the atom excitation reaction is of major concern, reactions were not given further consideration if no two adjacent transitions of this reaction have  $\Delta E$ 's which differ by at least one electron volt. The following reactions fall in this category.



Actually the krypton resonance reaction also falls in this category. However, in this case the results were plotted (see appendix C) using the value of  $E_1 = 200$  eV. These curves merely verify that experimental resolution between the transitions of the atom excitation reaction is impossible.

The other reactions containing krypton,



were plotted for  $E_1 = 200$  eV (see appendix C). The maximum difference of  $E_2$  between adjacent transitions of the atom excitation reaction is about 0.2 eV for the  $\text{He}^{4+} - \text{Kr}^{84}$  reaction and about 1.2 eV for the  $\text{A}^{40+} - \text{Kr}^{84}$  reaction. The former certainly cannot be resolved experimentally, and it is unlikely that the  $\text{A}^{40+} - \text{Kr}^{84}$  reaction can. This is neglecting the effects of the less abundant isotopes of krypton. If these are taken into account, it is felt that experimental resolution is impossible.

For some reactions the absolute value of the energy defect for the ion excitation reaction is greater than the absolute value of the energy defect (which will be called the ionization energy defect) for the ionization reaction.

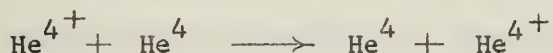


The value of  $\Delta E$  in this reaction is just the limiting absolute value of  $\Delta E$  for the atom excitation reaction. In these cases no information about the charge transfer cross section for the ion excitation reaction can be obtained, nor will the secondary ions caused by these transitions interfere with the resolution of transitions of the atom excitation reaction. Therefore, for these cases no ion excitation reactions are computed.

For the cases that the absolute value of the energy defects for ion excitation reactions are less than the absolute value of the ionization energy defect the ion excitation reactions are computed and plotted. However, even in these instances, it is quite possible that this reaction will

not interfere with resolution of the atom excitation transitions, since the cross section for ion excitation reactions is probably very small, as it would require the incident ion to interact with two electrons of the target atom. It would have to give energy to one electron to ionize the atom and to another electron to excite the resulting ion.

Each of the remaining reactions is considered individually. The curves which are plotted are in appendix C. A particular transition is specified as follows: The ground state reaction specifies a transition; a transition of the atom excitation reaction is specified by giving the excited state of the final atom; a transition of the ion excitation reaction is specified by giving the excited state of the secondary ion. The designation of excited states is that used in appendix A.



The maximum angle at which secondary ions from endothermic transitions are emitted is less than  $50^\circ$  when  $E_1$  is 20 or 100 eV.

Curves are plotted for  $E_1 = 200$  eV.

Reaction c is unimportant as the minimum absolute value of  $\Delta E$  for an ion excitation reaction is greater than the ionization energy defect.

It should be possible to distinguish the ground state reaction and the 2 energy state of the atom excitation reaction for  $E_1 = 200$  eV.



The maximum angle at which secondary ions from endothermic transitions are emitted is less than  $50^\circ$  when  $E_1$  is 20 eV. It is near  $50^\circ$  when  $E_1$  is 100 eV.

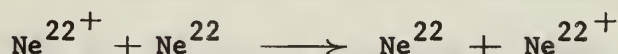
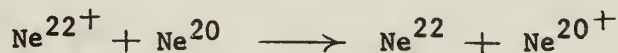
Curves are plotted for  $E_1 = 200$  eV.



Reaction c is unimportant as the minimum absolute value of  $\Delta E$  for an ion excitation reaction is greater than the ionization energy defect.

It is possible to resolve the ground state reaction.

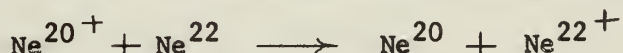
If it were not for the isotope  $\text{Ne}^{22}$  it should also be possible to distinguish the 3s state of the atom excitation reaction. However the presence of this isotope gives rise to the three additional reactions



For the first of these reactions the value of  $E_2$  differs only in the third decimal place from its value for the  $\text{Ne}^{20+} \text{---} \text{Ne}^{20}$  reaction and therefore can be neglected. The effect of the other two reactions is much greater, however. To see how important these effects are, the curves of



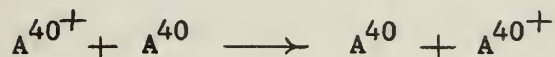
for the  $3s' (\frac{1}{2})^0$  atom excitation reaction ( $\Delta E = -16.844$  eV) and



for the  $3p (\frac{1}{2})$  atom excitation reaction ( $\Delta E = -18.377$  eV) are plotted on the same graph. It is coincidental that the values of  $E_2$  for these two transitions are identical to three significant figures. The curve of these two reactions falls approximately midway between those due to the  $3s' (\frac{1}{2})^0$  and  $3p (\frac{1}{2})$  atom excitation reactions of  $\text{Ne}^{20+} \text{---} \text{Ne}^{20}$  which it is desired to distinguish between. Furthermore, for the  $3s (1\frac{1}{2})$  atom excitation reaction of the  $\text{Ne}^{22+} \text{---} \text{Ne}^{20}$  reaction and for energy states slightly higher than the  $3p (\frac{1}{2})$  atom excitation reaction of the

$\text{Ne}^{20+} \longrightarrow \text{Ne}^{22}$  reaction the secondary ion is emitted with energies within the region being resolved. Thus resolution between these transitions will at least be very difficult.

The effect of the isotopes on the ground state reaction is quite small. This difference in  $E_2$  between these reactions and the primary reaction is less than 0.2 eV for all  $\theta$ 's less than  $50^\circ$ .



The maximum angle at which secondary ions from endothermic transitions are emitted is less than  $50^\circ$  when  $E_1$  is 20 eV.

Curves are plotted for  $E_1 = 100, 200$ , and 500 eV.

The minimum absolute value of  $\Delta E$  for an ion excitation reaction is not greater than the ionization energy defect. However, it is greater than the maximum absolute  $\Delta E$  of the atom excitation reactions being considered, and hence ion excitation reactions are of no concern.

It should be possible to distinguish the ground state reaction and the 4s state of the atom excitation reaction when  $E_1 = 100$  eV and possibly when  $E_1 = 200$  eV.



The maximum angle at which secondary ions from endothermic transitions are emitted is less than  $50^\circ$  when  $E_1$  is 20 eV.

Curves are plotted for  $E_1 = 100$  eV.

Reaction c is unimportant as the minimum absolute value of  $\Delta E$  for an ion excitation reaction is greater than the ionization energy defect.

It should be possible to distinguish the ground state reaction and the 2 energy state of the atom excitation reaction.

The effect of the reaction  $\text{He}^{4+} + \text{Ne}^{22} \longrightarrow \text{He}^4 + \text{Ne}^{22+}$  is shown on the graph. Although this isotope of neon gives quite different values  $E_2$  for small angles, the effect decreases for larger angles. In fact for endothermic reactions the two curves intersect. This intersection is in the region where detection would take place, so the effect of the isotope of neon is not a great hindrance in resolution of the states.



The maximum angle at which secondary ions from endothermic transitions are emitted is less than  $50^\circ$  when  $E_1$  is 20 eV.

Curves are plotted for  $E_1 = 100$  eV.

Ion excitation reactions have very low absolute values of  $\Delta E$  which must be considered.

In fact it seems that the only transitions which might be resolved are the 3p and 3d states of the ion excitation reaction. None of the atom excitation reactions can be distinguished.



The maximum angle at which secondary ions from endothermic transitions are emitted is less than  $50^\circ$  when  $E_1$  is 20, 100, or 200 eV.

Curves are plotted for  $E_1 = 500$  eV.

Reaction c is unimportant as the minimum absolute value of  $\Delta E$  for an ion excitation reaction is greater than the ionization energy defect.

It should be possible to distinguish the ground state reaction and the 3s atom excitation reaction.

The effect of the reaction  $\text{Ne}^{22+} + \text{He}^4 \longrightarrow \text{Ne}^{22} + \text{He}^{4+}$  is shown on the graph. The shift in  $E_2$  for the  $3s' (\frac{1}{2})^0$  atom excitation

reaction is so great as to move it out of the region of resolution.

Therefore, this will not in any way hinder resolution.



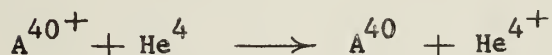
The maximum angle at which secondary ions from endothermic transitions are emitted is less than  $50^\circ$  when  $E_1 = 20$  eV.

Curves are plotted for  $E_1 = 100, 200,$  and  $500$  eV.

Ion excitation reactions have low absolute values of  $\Delta E$  which must be considered.

It should be possible to distinguish the ground state reaction, the 3s atom excitation reaction, and the 3p ion excitation reaction for  $E_1 = 100$  eV.

Two difficulties arise in resolving the 3s atom excitation reaction. The first is the effect of the isotope of neon giving rise to the reaction  $\text{Ne}^{22+} + \text{A}^{40} \longrightarrow \text{Ne}^{22} + \text{A}^{40+}$ . This is not serious, however, as the same comment applies that was made for the  $\text{He}^{4+} - \text{Ne}^{22}$  reaction. The second difficulty is that two transitions of the ion excitation reaction fall within this region. If the relative cross section of the ion excitation reaction to the atom excitation reaction is very small, as is likely, this also will not be important. If this is not true, resolution will probably be impossible.



The maximum angle at which secondary ions from endothermic reactions are emitted is less than  $50^\circ$  when  $E_1$  is 20, 200, or 500 eV.





The maximum angle at which secondary ions from endothermic transitions are emitted is less than  $50^\circ$  when  $E_1$  is 20 or 100 eV.

Curves are plotted for  $E_1 = 200$  eV.

Reaction c is unimportant as the minimum absolute value of  $\Delta E$  for an ion excitation reaction is greater than the ionization energy defect.

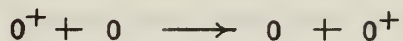
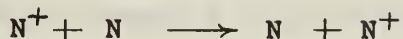
It is possible to resolve the ground state reaction.

It would be possible to resolve the 4s atom excitation reaction if it were not for  $Ne^{22}$ . As shown on the graph the 4p ( $\frac{1}{2}$ ) atom excitation reaction  $A^{40+} + Ne^{22} \longrightarrow A^{40} + Ne^{22+}$  gives higher values of  $E_2$  than the 4s' ( $\frac{1}{2}$ )<sup>o</sup> atom excitation reaction  $A^{40+} + Ne^{20} \longrightarrow A^{40} + Ne^{20+}$ . As the states above the 4p state are very close together, ions from the  $A^{40+} + Ne^{22}$  reaction of many of these states will fall within the region being resolved, making resolution difficult or impossible.

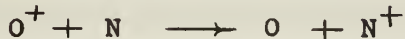
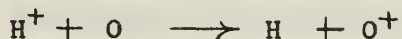
## 2.2 Hydrogen, Nitrogen, and Oxygen.

The possible transitions for each of the following reactions are now considered.

### Resonance reactions



### Non resonance reactions



Again only metastable states of the excited primary ion are considered. However, now both singly ionized nitrogen and oxygen have two metastable states, so that reactions e through h of page 2 cannot be disregarded. Furthermore, since the excitation energy of both the atom and the ion of these gases may be small, the absolute value of the energy defect of a reaction in which both final particles are left in an excited state (reaction d or h) is not necessarily large as was the case with the inert gases, and these reactions must be considered.

The energy defects were computed for transition of all reactions listed on page 2. For reactions in which the secondary ion is left in the ground state (reactions b and f) all transitions which left the final

atom in the lowest energy states were considered. Again the higher energy states were not considered because the difference in energy between succeeding energy states decreases as the excitation energy increases. The criteria as to where the cut-off in energy states occurred was that the difference in energy between any two remaining successive states did not exceed 0.2 electron volts. For the other types of reactions all transitions were considered which gave rise to energy defects which were less in absolute value than the ionization energy defects.

The computed energy defects for the reactions involving hydrogen, nitrogen, and oxygen are tabulated in appendix B.

If, for a reaction in which the primary ion is either nitrogen or oxygen, all of the transitions listed in appendix B must be considered, experimental resolution would be impossible. However, as with the inert gases it is likely that the cross section for reactions which leave the secondary ion in the excited state will be very low compared to those which leave the secondary ion in the ground state. An assumption to this effect was made so that  $E_2$  was calculated as a function of  $\theta$  for reactions a, b, e, and f only. The validity of this assumption can be tested experimentally from the inert gas reactions and from the present reactions in cases where the primary ion is hydrogen, since in both cases transitions considered are for reactions a, b, and e.

Using the values of  $\Delta E$  from appendix B, for the transitions to be considered,  $E_2$  was calculated as a function of  $\theta$  for each of the following values of  $E_1$ : 20 eV, 100 eV, 200 eV, 500 eV. The masses used were those of the most abundant isotope of each element. This is entirely satisfactory in all cases as the most abundant isotope accounts for

99.98% of hydrogen, 99.64% of nitrogen, and 99.76% of oxygen. Curves are given in appendix D of transitions for which resolution might be possible.

The effect of the value of  $E_1$  on the secondary ion is the same as it was for the inert gases as given on page 17. The minimum limiting value of  $E_1$  is again given by the maximum angle at which secondary ions in endothermic transitions are emitted, and again this value of  $\theta$  is arbitrarily taken to be  $50^\circ$ .

The determination as to which transitions of which reactions might be resolved experimentally can be made from the graphs of appendix D and considering the possible transitions of appendix B. Due regard should be given to the fact that the cross sections of some types of reactions are probably negligible.

The reactions of hydrogen, nitrogen, and oxygen are briefly summarized in table 1.

As a final remark, it is also noted that all the transitions considered for both the inert gases and hydrogen, oxygen, and nitrogen are kinematically possible. However, as  $\Delta E$  increases the ratio  $a|\Delta E|/(h\nu)$  increases, so that according to Massey /1/ adiabatic condition the charge transfer cross section probably decreases as the magnitude of the energy defect increases.



TABLE 1.  
Summary of Hydrogen, Nitrogen, and Oxygen Reactions.

Reaction	Values of $E_1$ for which the maximum angle at which secondary ions from endothermic transitions come off is less than 50°.	Values of $E_1$ for which curves are plotted.	Remarks
$H^+ + H \rightarrow H + H^+$	20 eV	100 eV, 200 eV	
$N^+ + N \rightarrow N + N^+$	None	20 eV, 100 eV	When $E_1$ is 20 eV, secondary ions are emitted at angles greater than 50° only when the final atom is left in the ground or a 2p state.
$O^+ + O \rightarrow O + O^+$	None	100 eV	Same as for $N^+ - N$ reaction.
$H^+ + N \rightarrow H + N^+$	20 eV	200 eV	Does not seem possible to resolve any of the transitions.
$H^+ + O \rightarrow H + O^+$	20 eV	None	The transitions are similar to those of the $H^+ - N$ reaction above. Since it does not seem possible to resolve any transitions, no curves were plotted.
$N^+ + H \rightarrow N + H^+$	20 eV	500 eV	When $E_1$ is 100 or 200 eV, secondary ions are emitted at angles greater than 50° only when the final atom is left in the ground or a 2p state.
$N^+ + O \rightarrow N + O^+$	None	200 eV	Same as for $N^+ - N$ reaction.
$O^+ + H \rightarrow O + H^+$	20 eV	None	Same as for $N^+ - H$ reaction. The situation is similar to that of the $N^+ - H$ reaction and no graphs are drawn.
$O^+ + N \rightarrow O + N^+$	None	None	Same as for $N^+ - N$ reaction.

### 3. Nonstationary Target Atoms.

The previous work has assumed the initial atom to be at rest. Experimentally this will not be the case, so the effect of the motion of the initial atom will now be considered. If the initial atoms are those of a gas contained in a cell they would have a Maxwell-Boltzman distribution of velocity. Using this velocity distribution of the initial atom, it was attempted to determine the distribution of the secondary ion. The mathematics became involved, and it was decided not to pursue this problem at this time. Instead the actual experimental problem of collimating the initial atoms into a molecular beam was considered.

The collision process is now shown in figure 8, where the initial atoms have velocities in the positive  $y$  direction.

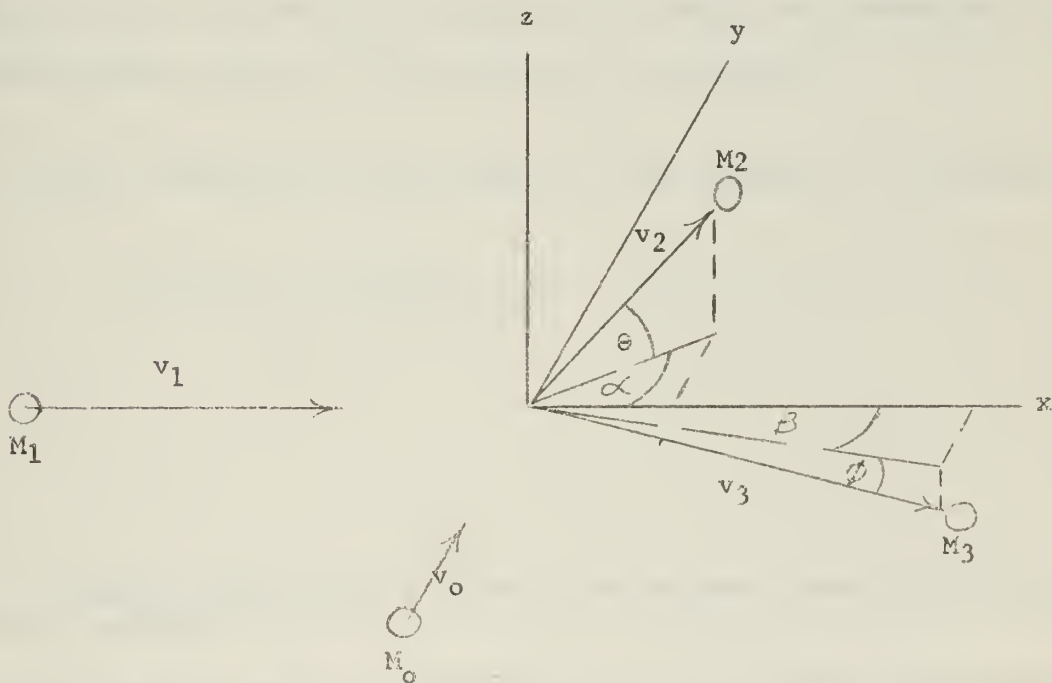


Figure 8.  
Collision process when the initial atoms have a Maxwellian speed distribution in the positive  $y$  direction.

According to F. Hurlbut<sup>2</sup> if the Knudsen number<sup>3</sup> is greater than 100 the probability distribution in speed of the initial atoms is given by

$$P(v_0) = \frac{2}{a^4} v_0^3 \exp \left[ -\frac{v_0^2}{a^2} \right] \quad \text{where} \quad a = \left[ \frac{2kT}{M_0} \right]^{1/2}$$

Then, for a fixed  $E_2$ , the angular distribution of the secondary ion is given by /4/

$$11) \quad P(\theta)_{v_1, v_2, \alpha = \text{const.}} = P(v_0) \frac{dv_0}{d\theta} \quad \text{or}$$

$$12) \quad P(\theta)_{v_1, v_2, \alpha = \text{const.}} = \frac{2}{a^4} v_0^3 \exp \left[ -\frac{v_0^2}{a^2} \right] \frac{dv_0}{d\theta}$$

$v_0$  can be found as a function of  $v_2, \theta$ , and the fixed parameters of equation 12 by conservation of momentum and energy considerations of the system shown in figure 8. This results in the equation

$$13) \quad (M_3 + M_2)M_2 v_2^2 + (M_1 - M_3)M_1 v_1^2 + (M_0 - M_3)M_0 v_0^2 - 2M_3 \Delta E \\ = 2M_2 v_2 \cos \theta (M_0 v_0 \sin \alpha + M_1 v_1 \cos \alpha)$$

<sup>2</sup>Private Communication from Dr. Frank Hurlbut, University of California, Berkeley.

<sup>3</sup>The Knudsen number is defined as the ratio of the mean free path of the atoms to the diameter of the collimating tube opening. For the experiment proposed an order of magnitude calculation of the Knudsen number gives a value of 1000.

or solving for  $v_0$  explicitly

$$\begin{aligned}
 14) \quad v_0 = & - \frac{2 M_0 M_2 v_2 \cos \theta \sin \alpha}{2 M_0 (M_3 - M_0)} \\
 & \pm \left\{ [2 M_0 M_2 v_2 \cos \theta \sin \alpha]^2 - 4 M_0 (M_3 - M_0) [M_1 (M_3 - M_1) v_1^2 - M_2 (M_3 + M_2) v_2^2 \right. \\
 & \left. + 2 M_1 M_2 v_1 v_2 \cos \theta \cos \alpha + 2 M_3 \Delta E] \right\}^{1/2} / [2 M_0 (M_3 - M_0)]
 \end{aligned}$$

It is seen that  $v_0$  is double valued. When  $v_2$  is fixed, the equations leading to equation 14 can be reduced to that of a hyperbola and that of a straight line, so that the double valuedness of  $v_0$  is not due to the introduction of an extraneous root. Thus there are two values of  $v_0$  which give rise to the same velocity,  $v_2$ , of the secondary ion, and thus two angular distributions of the secondary ions for each fixed value of  $E_2$ ; one arising from the probability distribution of each value of  $v_0$  which gives rise to the same  $v_2$ . Mathematically there is no restriction on the sign of  $v_0$ ; i.e. both values of  $v_0$  may be positive, both may be negative, or one may be positive and one negative. Physically, however, no initial atoms have velocities in the negative  $y$  direction so that only positive values of  $v_0$  give rise to distribution probabilities of the secondary ions which are not everywhere zero. In the case that both values of  $v_0$  are positive, the observed probability density of the secondary ions is the sum of the two computed probability densities.

The relative distribution in angle  $\theta$  at which secondary ions are emitted with values of  $\alpha$  of  $1^\circ$ , and  $0^\circ$ , and  $-1^\circ$  for some of the reactions



shown in appendix C are plotted in appendix E. The following observations are noted, where in the following discussion the angle of emission of the secondary ion with a given energy when  $v_0$  is equal to zero will be denoted by  $\theta_0$ .

1. In the case of  $\alpha = 0$ ; if  $M_3 > M_0$  all the secondary ions of a given energy will be emitted at angles greater than  $\theta_0$ , i.e. the distribution is all above the angle it was calculated the secondary ion would be emitted at assuming  $v_0 = 0$ ; if  $M_3 < M_0$  the secondary ions of a given energy will be emitted at angles smaller than  $\theta_0$ , i.e. the distribution is all below the angle it was calculated the secondary ion would be emitted at assuming  $v_0 = 0$ . That this should be the case mathematically can be seen by rewriting equation 13.

$$15) \quad \cos \theta = \frac{(M_0 - M_3)E_0 + (M_3 + M_2)E_2 + (M_1 - M_3)E_1 - M_3 \Delta E}{M_0 M_2 v_0 v_2 \sin \alpha + M_1 M_2 v_1 v_2 \cos \theta}$$

When  $\alpha = 0$  the only dependence on the speed of the initial atom is the first term in the numerator. The initial calculations of  $\theta$  were made assuming  $E_0 = 0$ . Now if values of  $E_0$  (which must be positive) are inserted in equation 15; if  $M_3 > M_0$ ,  $\cos \theta$  will decrease, giving greater values of  $\theta$ ; and the distribution of  $E_0$  will give a distribution of secondary ions all emitted at values of  $\theta$  greater than  $\theta_0$ ; if  $M_3 < M_0$ ,  $\cos \theta$  will increase and the value of  $\theta$  will decrease and the distribution of  $E_0$  will give a distribution of secondary ions all emitted at values of  $\theta$  smaller than  $\theta_0$ .  $M_3 = M_0$  is the limiting case of both of the above cases. In this case equation 15 indicates that the secondary ions are emitted at the angle calculated assuming  $E_0 = 0$ .

It can be shown that the above distributions are also physically plausible by considering the energy of the initial ion as a perturbation on the initial case where  $E_0 = 0$ . Thus the initial system has additional energy  $E_0$ , and we ask how does this affect the final system.

$$\text{Since } \alpha = 0, \quad M_0 v_0 = M_3 v_{3y}$$

Hence, the final atom acquires a component of velocity in the y direction of  $v_{3y} = (M_0/M_3)v_0$ . If, to a first approximation, its velocity in the x-z plane remains unchanged from that it had when  $E_0 = 0$ , the increase in energy of the final ion is  $\Delta E_3 = (M_0 v_0)^2 / (2 M_3)$ . The ratio of the added initial energy,  $E_0$ , to the increase in energy of the final atom is

$$\frac{E_0}{\Delta E_3} = \frac{M_3}{M_0}$$

$$\text{or} \quad \Delta E_3 = \frac{M_0}{M_3} E_0$$

Hence, if  $M_3 > M_0$ , then  $\Delta E_3 < E_0$  and some of the additional energy  $E_0$  is acquired by  $E_2$ . Therefore, according to the curves of appendix C or D the particle would be emitted at an angle smaller than  $\theta_0$ . However, we are looking at a fixed  $E_2$ , so that particles which had a smaller value of  $E_2$  and hence a greater  $\theta$  in the original case will now come out with the fixed value of energy. The opposite argument shows that the secondary ions will be emitted with decreased values of  $\theta$  when  $M_3 < M_0$ . When  $M_3 = M_0$ , all the initial energy will go to increase the energy of the final atom leaving the secondary ion unaffected as was concluded above.

2. If  $\alpha$  is not equal to zero, and if  $\theta < 90^\circ$ , the point at which the probability distribution goes to zero is shifted to a value of  $\theta$  which is lower than it was when  $\alpha = 0$ . Thus, in the case that  $M_3 > M_0$

the distribution curve of the secondary ions includes  $\theta_0$ ; whereas when  $M_3 < M_0$  the distribution curve of the secondary ion is now completely beyond  $\theta_0$ . However, for the values of  $\alpha$  considered ( $\alpha = 1^\circ$  and  $-1^\circ$ ) this shift is a maximum of  $0.002^\circ$  and hence is unimportant. Also, as seen in appendix D the relative probabilities of a secondary ion emitted at an angle  $\theta$  for the values of  $\alpha = 1, 0$ , and  $-1$  degrees are such that the distribution of  $\alpha = 0$  is an approximate average of the three. Therefore, it is concluded that the distribution function when  $\alpha = 0$  should be an approximately average distribution function for a small increment of angle  $\alpha$  centered on  $\alpha = 0$ .

3. The maximum probability density occurs at angles close to  $\theta_0$ . In the cases considered in appendix E, the greatest difference between the angle at which the probability density is a maximum and  $\theta_0$  is less than  $0.05^\circ$ .

4. The fixed value of  $v_2$  or  $E_2$  being considered has a marked effect on the probability distribution. As the value of  $E_2$  is increased, the maximum probability density occurs at angles nearer  $\theta_0$ , and the distribution curve is less spread out.

5. In agreement with equation 15 the spread in distribution of the secondary ions decreases as the difference in magnitude between  $M_3$  and  $M_0$  decreases.

6. Increasing the absolute value of  $\Delta E$  increases the spread in distribution of the secondary ions. This effect is not great however.

## BIBLIOGRAPHY

1. H. S. W. Massey and E. H. S. Burhop, *Electronic and Ionic Impact Phenomena*, Oxford Univ. Press, 1952, Chapters VII, VIII.
2. J. B. Hasted, *Charge Transfer and Collisional Detachment*, Atomic and Molecular Processes, edited by D. R. Bates, Academic Press, pp 697-720, 1962.
3. N. V. Fedorenko, *Ionization in Collisions Between Ions and Atoms*, Soviet Physics, Uspekhi Vol. 2 (68), 526, 1959.
4. E. Parzen, *Modern Probability Theory and its Applications*, John Wiley & Sons, Inc., 1960, Chapter 7.
5. *Atomic Energy Levels as Derived from the Analysis of Optical Spectra*, United States Department of Commerce, National Bureau of Standards, Circular 467, Vol. I, II.

## APPENDIX A

### COMPUTED VALUES OF THE ENERGY DEFECT FOR CHARGE TRANSFER REACTIONS OF INERT GASES

The energy levels of the excited state of the atoms and ions are taken from Atomic Energy Levels /5/. The notation used to designate the energy state of an atom or ion is the spectroscopic notation used in this publication except that the ground state is designated as such instead of using the spectroscopic designation.

For inert gas reactions only the final atom and the secondary ion are in states other than the ground state. Therefore, in the tables below AI and BII are the final atom and the secondary ion respectively, and the energy defects tabulated are for transitions from the ground state of the primary ion and excited atom to the listed states of the final atom and the secondary ion.

All of the lowest excited states of the final atom and the secondary ion are listed. However, values of the energy defect which are greater than the ionization energy defect are not shown except for the ones which indicate that this is true for all others. The values of the energy defects are in units of electron volts. Metastable states of the final atom are shown by an asterisk.

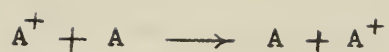




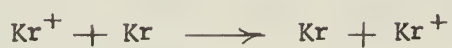
HeI/HeII	Ground	2s 2S & 2p 2P <sup>o</sup>
Ground	0.000	-40.80
2s 3S *	-19.813	
2s 1S *	-20.609	
2p 3P <sup>o</sup>	-20.956	
2p 1P <sup>o</sup>	-21.211	
3s 3S	-22.711	
3s 1S	-22.913	
3p 3P <sup>o</sup>	-23.000	
3d 3D	-23.067	
3d 1D	-23.067	
3p 1P <sup>o</sup>	-23.080	
4s 3S	-25.587	
Ionization	-24.580	



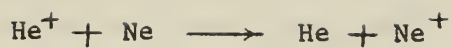
NeI/NeII	Ground	2p <sup>6</sup> 2S
Ground	0.000	-26.90
3s (1½) <sup>o</sup> *	-16.615	
3s' (½) <sup>o</sup> *	-16.711	
3s' (½) <sup>o</sup>	-16.844	
3p (½)	-18.377	
3p (2½)	-18.56	
3p (1½)	-18.62	
3p (½)	-18.71	
3p' (1½)	-18.69	
3p' (½)	-18.8	
4s (1½) <sup>o</sup>	-19.66	
Ionization	-21.559	



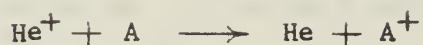
AI/AII	Ground	$3p^6 \ ^2S$	$3d \ ^4D$
Ground	- 0.000	-13.476	-16.42
$4s \ (1\frac{1}{2})^0 *$	-11.545	-25.021	
$4s \ (1\frac{1}{2})^0$	-11.621		
$4s' \ (\frac{1}{2})^0 *$	-11.719		
$4s' \ (\frac{1}{2})^0$	-11.817		
$4p \ (\frac{1}{2})$	-12.903		
$4p \ (2\frac{1}{2})$	-13.08		
$4p \ (1\frac{1}{2})$	-13.15		
$4p \ (\frac{1}{2})$	-13.27		
$4p' \ (1\frac{1}{2})$	-13.29		
$4p' \ (\frac{1}{2})$	-13.40		
$3d \ (\frac{1}{2})^0$	-13.85		
Ionization	-15.755		



KrI/KrII	Ground	$4p^6 \ ^2S$	$5s \ ^4P$
Ground	0.000	-13.51	-14.27
$5s \ (1\frac{1}{2})^0 *$	- 9.913		
$5s \ (1\frac{1}{2})^0$	-10.030		
$5s' \ (0\frac{1}{2})^0 *$	-10.559		
$5s' \ (0\frac{1}{2})^0$	-10.641		
$5p \ (0\frac{1}{2})$	-11.30		
$5p \ (2\frac{1}{2})$	-11.44		
Ionization	-13.996		



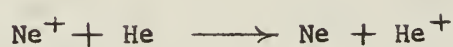
HeI/NeII	Ground	$2p^6 2s$
Ground	3.021	-23.882
$2s 3s *$	-16.792	
$2s 1s *$	-17.588	
$2p 3p^o$	-17.935	
$2p 1p^o$	-18.190	
$3s 3s$	-19.690	
$3s 1s$	-19.892	
$3p 3p^o$	-19.979	
$3d 3d$	-20.046	
$3d 1d$	-20.046	
$3p 1p^o$	-20.059	
$4s 3s$	-20.566	
Ionization	-21.559	



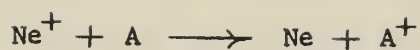
HeI/AII	Ground	$3p^6 2s$	$3d 4d$	$4s 4p$	$4s 2p$	$3d 4f$	$3d 2p$	$3d 4p$	$4s'' 2s$
Ground	8.825	- 4.65	- 7.60	-7.91	-8.37	-8.88	-9.16	-9.46	-11.91
$2s 3s *$	-10.988	-15.64	-18.59						
$2s 1s *$	-11.784	-16.43							
$2p 3p^o$	-12.131								
$2p 1p^o$	-12.386								
$3s 3s$	-13.886								
$3s 1s$	-14.088								
$3p 3p^o$	-14.175								
$3d 3d$	-14.242								
$3d 1d$	-14.242								
$3p 1p^o$	-14.255								
$4s 3s$	-14.762								
Ionization	-15.755								



HeI/KrII	Ground	4p <sup>6</sup> 2S	5s 4P	5s 2P	4d 4D	4d 4F	5s' 2D	4d 4P
Ground	10.584	-2.93	-3.69	-4.26	-4.42	-5.29	-5.25	-5.65
2s 3S *	- 9.229	-22.74						
2s 1S *	-10.025							
2p 3P <sup>o</sup>	-10.372							
2p 1P <sup>o</sup>	-10.627							
3s 3S	-12.127							
3s 1S	-12.329							
3p 3P <sup>o</sup>	-12.416							
3d 3D	-12.483							
3d 1D	-12.483							
3p 1P <sup>o</sup>	-12.496							
4s 3S	-13.003							
Ionization	-13.996							



NeI/HeII	Ground	2s 2S & 2p 2P <sup>o</sup>
Ground	- 3.021	-43.82
3s (1½) <sup>o</sup> *	-19.636	
3s' (½) <sup>o</sup> *	-19.732	
3s' (½) <sup>o</sup>	-19.865	
3p (½)	-21.398	
3p (2½)	-21.58	
3p (1½)	-21.64	
3p (½)	-21.73	
3p' (1½)	-21.71	
3p' (½)	-21.8	
4s (1½) <sup>o</sup>	-22.68	
Ionization	-24.580	



NeI/AII	Ground	$3p^6 \ 2S$	$3d \ 4D$	$4s \ 4P$	$4s \ 2P$	$3d \ 4F$	$3d \ 2P$	$3d \ 4P$	$4s'' \ 2S$
Ground	5.804	-7.67	-10.62	-10.93	-11.39	-11.90	-12.18	-12.48	-14.93
$3s \ (1\frac{1}{2})^0 *$	-10.811	-24.29							
$3s' \ (\frac{1}{2})^0 *$	-10.907								
$3s' \ (\frac{1}{2})^0$	-11.040								
$3p \ (\frac{1}{2})$	-12.573								
$3p \ (2\frac{1}{2})$	-12.75								
$3p \ (1\frac{1}{2})$	-12.81								
$3p \ (\frac{1}{2})$	-12.90								
$3p' \ (1\frac{1}{2})$	-12.89								
$3p' \ (1\frac{1}{2})$	-13.0								
$4s \ (1\frac{1}{2})^0$	-13.86								
Ionization	-15.755								



NeI/KrII	Ground	$4p^6 \ 2S$	$5s \ 4P$	$5s \ 2P$	$4d \ 4D$	$4d \ 4F$	$5s' \ 2D$	$4d \ 4P$
Ground	7.563	-5.95	-6.71	-7.28	-7.44	-8.31	-8.27	-8.67
$3s \ (1\frac{1}{2})^0 *$	- 9.052	-22.56						
$3s' \ (\frac{1}{2})^0 *$	- 9.148							
$3s' \ (\frac{1}{2})^0$	- 9.281							
$3p \ (\frac{1}{2})$	-10.814							
$3p \ (2\frac{1}{2})$	-10.99							
$3p \ (1\frac{1}{2})$	-11.05							
$3p \ (\frac{1}{2})$	-11.14							
$3p' \ (1\frac{1}{2})$	-11.13							
$3p' \ (\frac{1}{2})$	-11.2							
$4s \ (1\frac{1}{2})^0$	-12.10							
Ionization	-13.996							

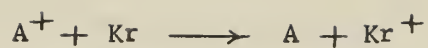




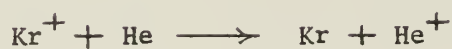
AI/HeII	Ground	$2s\ 2S$ & $2p\ 2P^0$
Ground	- 8.825	-49.63
$4s\ (1\frac{1}{2})^0 *$	-20.370	
$4s\ (1\frac{1}{2})^0$	-20.440	
$4s'\ (\frac{1}{2})^0$	-20.544	
$4s'\ (\frac{1}{2})^0$	-20.642	
$4p\ (\frac{1}{2})$	-21.728	
$4p\ (2\frac{1}{2})$	-21.91	
$4p\ (1\frac{1}{2})$	-21.98	
$4p\ (\frac{1}{2})$	-22.10	
$4p'\ (1\frac{1}{2})$	-22.12	
$4p'\ (\frac{1}{2})$	-22.23	
$3d\ (\frac{1}{2})^0$	-22.68	
Ionization	-24.580	



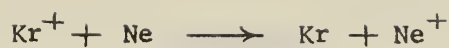
AI/NeII	Ground	$2p^6\ 2S$
Ground	- 5.804	-32.70
$4s\ (1\frac{1}{2})^0 *$	-17.349	
$4s\ (1\frac{1}{2})^0$	-17.425	
$4s'\ (\frac{1}{2})^0 *$	-17.523	
$4s'\ (\frac{1}{2})^0$	-17.621	
$4p\ (\frac{1}{2})$	-18.707	
$4p\ (2\frac{1}{2})$	-18.88	
$4p\ (1\frac{1}{2})$	-18.95	
$4p\ (\frac{1}{2})$	-19.07	
$4p'\ (1\frac{1}{2})$	-19.09	
$4p'\ (\frac{1}{2})$	-19.20	
$3d\ (\frac{1}{2})^0$	-19.65	
Ionization	-21.559	



AI/KrII	Ground	$4p^6 \ 2S$	$5s \ 4P$	$5s \ 2P$	$4d \ 4D$	$4d \ 4F$
Ground	1.76	-11.75	-12.51	-13.08	-13.24	-14.11
$4s \ (1\frac{1}{2})^0 *$	-9.79	-24.30				
$4s \ (1\frac{1}{2})^0$	-9.86					
$4s' \ (\frac{1}{2})^0 *$	-9.96					
$4s' \ (\frac{1}{2})^0$	-10.06					
$4p \ (\frac{1}{2})$	-11.14					
$4p \ (2\frac{1}{2})$	-11.32					
$4p \ (1\frac{1}{2})$	-11.39					
$4p \ (\frac{1}{2})$	-11.51					
$4p' \ (1\frac{1}{2})$	-11.53					
$4p' \ (\frac{1}{2})$	-11.64					
$3d \ (\frac{1}{2})^0$	-12.11					
Ionization	-13.996					



KrI/HeII	Ground	$2s \ 2S \ \& \ 2p \ 2P$
Ground	-10.58	-30.40
$5s \ (1\frac{1}{2})^0 *$	-20.49	
$5s \ (1\frac{1}{2})^0$	-20.61	
$5s' \ (0\frac{1}{2})^0 *$	-21.14	
$5s' \ (0\frac{1}{2})^0$	-21.22	
$5p \ (0\frac{1}{2})$	-21.88	
$5p \ (2\frac{1}{2})$	-22.03	
Ionization	-24.580	



KrI/NeII	Ground	$2p^6 \ 2s$
Ground	-7.56	-34.47
5s $(1\frac{1}{2})^{\circ} *$	-17.47	
5s $(1\frac{1}{2})^{\circ}$	-17.59	
5s' $(0\frac{1}{2})^{\circ} *$	-18.12	
5s' $(0\frac{1}{2})^{\circ}$	-18.2	
5p $(0\frac{1}{2})$	-18.86	
5p $(2\frac{1}{2})$	-19.00	
Ionization	-21.559	



KrI/AII	Ground	$3p^6 \ 2s$	$3d \ 4d$
Ground	-1.76	-15.24	-18.18
5s $(1\frac{1}{2})^{\circ} *$	-11.67	-25.15	
5s $(1\frac{1}{2})^{\circ}$	-11.79		
5s' $(0\frac{1}{2})^{\circ} *$	-12.32		
5s' $(0\frac{1}{2})^{\circ}$	-12.40		
5p $(0\frac{1}{2})$	-13.06		
5p $(2\frac{1}{2})$	-13.20		
Ionization	-15.755		

## APPENDIX B

### COMPUTED VALUES OF THE ENERGY DEFECT FOR CHARGE TRANSFER REACTIONS OF HYDROGEN, NITROGEN, AND OXYGEN

The energy levels of the excited state of the atoms and ions are taken from Atomic Energy Levels. The notation used to designate the energy state of an atom or ion is the spectroscopic notation used in this publication except that the ground state is designated as such instead of using the spectroscopic designation.

Singly ionized nitrogen and oxygen each have two metastable states. Therefore, for each reaction in which the primary ion is either nitrogen or oxygen and the initial atom is not hydrogen three tables are given; one for the primary ion in the ground state and one for each of the metastable states of the primary ion. Within the tables the states listed, AI and BII, are of the final atom and the secondary ion respectively. The states are listed in the same way for reactions in which hydrogen is the primary ion, but here, since  $H^+$  has no metastable states (no excited states) only one table is necessary for each reaction.

If hydrogen is the initial atom, the final ion is  $H^+$  which of course can not have excited states. Hence, for reactions in which nitrogen or oxygen is the primary ion and hydrogen is the initial atom only one table is needed for each reaction in which the energy states listed, AI and AII, are those of the final atom and the metastable states of the primary ion respectively.

All of the lowest excited states of the final atom and secondary ion are listed. However, values of the energy defect which are greater than the ionization energy defect are not shown except for the ones which indicate that this is the case for all others. The values of the energy defects are in units of electron volts. Metastable states of the final atom and secondary ion are shown by an asterisk.



HI/HII	Ground
Ground	0.000
2s <sup>2</sup> S	-10.196
2p <sup>2</sup> P <sup>o</sup>	
3s <sup>2</sup> S	-12.084
3p <sup>2</sup> P <sup>o</sup>	
3d <sup>2</sup> D	
4s <sup>2</sup> S	-12.745
4p <sup>2</sup> P <sup>o</sup>	
4d <sup>2</sup> D	
4f <sup>2</sup> F <sup>o</sup>	
5s <sup>2</sup> S	-13.051
etc.	
6s <sup>2</sup> S	-13.217
etc.	



Primary ion in ground state

NI/NII	Ground	2p <sup>2</sup> <sup>1</sup> D*	2p <sup>2</sup> <sup>1</sup> S*	2p <sup>3</sup> <sup>5</sup> S <sup>o</sup>	2p <sup>3</sup> <sup>3</sup> D <sup>o</sup>	2p <sup>3</sup> <sup>3</sup> P <sup>o</sup>	2p <sup>3</sup> <sup>1</sup> D <sup>o</sup>
Ground	0.000	-1.90	-4.05	-5.85	-11.43	-13.54	-17.87
2p <sup>3</sup> <sup>2</sup> D <sup>o</sup> *	-2.383	-4.28	-6.43	-8.23	-13.81	-15.92	
2p <sup>3</sup> <sup>2</sup> P <sup>o</sup> *	-2.831	-4.73	-6.88	-8.68	-14.26		
3s <sup>4</sup> P	-10.33	-12.23	-14.38	-16.18			
3s <sup>2</sup> P	-10.68	-12.58	-14.73				
3p <sup>4</sup> S <sup>o</sup>	-11.99	-13.89					
3p <sup>2</sup> D <sup>o</sup>	-12.00	-13.90					
3p <sup>2</sup> P <sup>o</sup>	-12.12	-14.02					
3s' <sup>2</sup> D	-12.35	-14.25					
4s <sup>4</sup> P	-12.85	-14.75					
Ionization	-14.54						



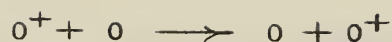


Primary ion in  $2p^2 \ 1D$  state

NI/NII	Ground	$2p^2 \ 1D^*$	$2p^2 \ 1S^*$	$2p^3 \ 5S^o$	$2p^3 \ 3D^o$	$2p^3 \ 3P^o$	$2p^3 \ 1D^o$
Ground	1.90	0.00	-2.15	-3.95	-9.53	-11.64	-15.97
$2p^3 \ 2D^o^*$	-0.48	-2.38	-4.53	-6.33	-11.91	-14.02	
$2p^3 \ 2P^o^*$	-0.93	-2.83	-4.98	-6.78	-12.36		
$3s \ 4P$	-8.43	-10.33	-12.48	-14.28			
$3s \ 2P$	-8.78	-10.68	-12.83				
$3p \ 4S^o$	-10.09	-11.99					
$3p \ 2D^o$	-10.10	-12.00					
$3p \ 2P^o$	-10.22	-12.12					
$3s' \ 2D$	-10.45	-12.35					
$4s \ 4P$	-10.95	-12.85					
Ionization	-12.64						

Primary ion in  $2p^2 \ 1S$  state

NI/NII	Ground	$2p^2 \ 1D^*$	$2p^2 \ 1S^*$	$2p^3 \ 5S^o$	$2p^3 \ 3D^o$	$2p^3 \ 3P^o$	$2p^3 \ 1D^o$
Ground	4.05	2.15	0.00	-1.80	-7.38	-9.49	-13.82
$2p^3 \ 2D^o^*$	1.67	-0.23	-2.38	-4.18	-9.76	-11.87	
$2p^3 \ 2P^o^*$	1.22	-0.68	-2.83	-4.63	-10.21		
$3s \ 4P$	-6.28	-8.18	-10.33	-12.13			
$3s \ 2P$	-6.63	-8.53	-10.68				
$3p \ 4S^o$	-7.94	-9.84					
$3p \ 2D^o$	-7.95	-9.85					
$3p \ 2P^o$	-8.07	-9.97					
$3s' \ 2D$	-8.30	-10.20					
$4s \ 4P$	-8.80	-10.70					
Ionization	-10.49						

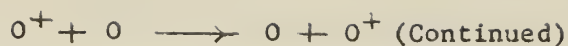


Primary ion in ground state

OI/OII	Ground	$2p^3 \ 2D^o *$	$2p^3 \ 2P^o *$	$2p^4 \ 4P$
Ground	0.000	-3.32	-5.02	-14.84
$2p^4 \ 1D *$	-1.967	-5.29	-6.99	
$2p^4 \ 1S *$	-4.189	-7.51	-9.21	
$3s \ 5S^o$	-9.144	-12.46	-14.16	
$3s \ 3S^o$	-9.519	-12.84		
$3p \ 5P$	-10.738	-14.06		
$3p \ 3P$	-10.986			
$4s \ 5S^o$	-11.843			
$3s' \ 1D^o$	-12.725			
$4d \ 5D^o$	-12.750			
$4d \ 3D^o$	-12.755			
$5p \ 3P$	-12.876			
$6s \ 5S^o$	-13.017			
Ionization	-13.614			

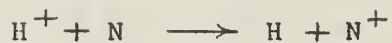
Primary ion in  $2p^3 \ 2D^o$  metastable state

OI/OII	Ground	$2p^3 \ 2D^o *$	$2p^3 \ 2P^o *$	$2p^4 \ 4P$
Ground	3.32	0.00	-1.70	-11.52
$2p^4 \ 1D *$	1.35	-1.97	-3.67	
$2p^4 \ 1S *$	-0.87	-4.19	-5.89	
$3s \ 5S^o$	-5.82	-9.14	-10.84	
$3s \ 3S^o$	-6.20	-9.52		
$3p \ 5P$	-7.42	-10.74		
$3p \ 3P$	-7.67			
$4s \ 5S^o$	-8.52			
$3s' \ 1D^o$	-9.41			
$4d \ 5D^o$	-9.43			
$4d \ 3D^o$	-9.44			
$5p \ 3P$	-9.56			
$6s \ 5S^o$	-9.70			
Ionization	-10.29			



Primary ion in  $2p^3 2p^o$  metastable state

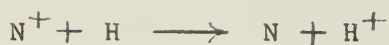
OI/OII	Ground	$2p^3 2D^o *$	$2p^3 2P^o *$	$2p^4 4P$
Ground	5.02	1.70	0.00	-9.82
$2p^4 1D^o *$	3.05	-0.27	-1.97	
$2p^4 1S *$	0.83	-2.49	-4.19	
$3s 5S^o$	-4.12	-7.44	-9.14	
$3s 3S^o$	-4.50	-7.82		
$3p 5P$	-5.72	-9.04		
$3p 3P$	-5.97			
$4s 5S^o$	-6.82			
$3s' 1D^o$	-7.71			
$4d 5D^o$	-7.73			
$4d 3D^o$	-7.74			
$5p 3P$	-7.86			
$6s 5S^o$	-8.00			
Ionization	-8.59			



HI/NII	Ground	$2p^2 1D *$	$2p^2 1S *$	$2p^3 5S^o$	$2p^3 3D^o$	$2p^3 3P^o$	$2p^3 1D^o$
Ground	-0.94	-2.84	-4.99	-6.79	-12.37	-14.48	-18.81
$2s 2S$	-11.14	-13.04	-15.19				
$2p 2P^o$							
$3s 2S$	-13.02	-14.92					
$3p 2P^o$							
$3d 2D$							
$4s 2S$	-13.69						
$4p 2P^o$							
$4d 2D$							
$4f 2F^o$							
$5s 2S$	-13.99						
etc.							
$6s 2S$	-14.16						
etc.							
Ionization	-14.54						



HI/OII	Ground	$2p^3 \ 2D^{\circ} *$	$2p^3 \ 2P^{\circ} *$	$2p^4 \ 4P$
Ground	-0.019	-3.34	-5.04	-14.86
$2s \ 2S$	-10.215	-13.64		
$2p \ 2P$				
$3s \ 2S$	-12.103			
$3p \ 2P^{\circ}$				
$3d \ 2D$				
$4s \ 2S$	-12.764			
$4p \ 2P^{\circ}$				
$4d \ 2D$				
$4f \ 2F^{\circ}$				
$5s \ 2S$	-13.070			
etc.				
$6s \ 2S$	-13.236			
etc.				
Ionization	-13.614			



NI/NII	Ground	$2p^2 \ 1D *$	$2p^2 \ 1S *$
Ground	0.94	2.84	4.99
$2p^3 \ 2L^{\circ} *$	-1.44	0.46	2.61
$2p^3 \ 2P^{\circ} *$	-1.89	0.01	2.16
$3s \ 4P$	-9.39	-7.49	-5.34
$3s \ 2P$	-9.74	-7.84	-5.69
$3p \ 4S^{\circ}$	-11.05	-9.15	-7.00
$3p \ 2D^{\circ}$	-11.06	-9.16	-7.01
$3p \ 2P^{\circ}$	-11.18	-9.28	-7.13
$3s' \ 2D$	-11.41	-9.51	-7.36
$4s \ 4P$	-11.91	-10.01	-7.86
Ionization	-13.60		



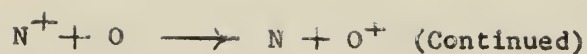
Primary ion in ground state

NI/OII	Ground	$2p^3 \ 2D^{\circ} *$	$2p^3 \ 2P^{\circ} *$	$2p^4 \ 4P$
Ground	0.93	-2.39	-4.09	-13.91
$2p^3 \ 2D^{\circ} *$	-1.45	-4.77	-6.47	
$2p^3 \ 2P^{\circ} *$	-1.90	-5.22	-6.92	
$3s \ 4P$	-9.40	-12.72	-13.42	
$3s \ 2P$	-9.75	-13.07	-13.77	
$3p \ 4S^{\circ}$	-11.03	-14.35		
$3p \ 2D^{\circ}$	-11.07			
$3p \ 2P^{\circ}$	-11.19			
$3s' \ 2D$	-11.42			
$4s \ 4P$	-11.92			
Ionization	-13.61			

Primary ion in  $2p^2 \ 1D$  metastable state

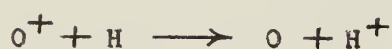
NI/OII	Ground	$2p^3 \ 2D^{\circ} *$	$2p^3 \ 2P^{\circ} *$	$2p^4 \ 4P$
Ground	2.83	-0.49	-2.19	-12.01
$2p^3 \ 2D^{\circ} *$	0.45	-2.87	-4.57	
$2p^3 \ 2P^{\circ} *$	0.00	-3.32	-5.02	
$3s \ 4P$	-7.50	-10.82	-11.52	
$3s \ 2P$	-7.85	-11.17	-11.87	
$3p \ 4S^{\circ}$	-9.13	-12.45		
$3p \ 2D^{\circ}$	-9.17			
$3p \ 2P^{\circ}$	-9.29			
$3s' \ 2D$	-9.52			
$4s \ 4P$	-10.02			
Ionization	-11.71			





Primary ion in  $2p^2 1s$  metastable state

NI/OII	Ground	$2p^3 2D^o *$	$2p^3 2P^o *$	$2p^4 4p$
Ground	3.12	1.66	-0.04	-9.86
$2p^3 2D^o *$	2.60	-0.72	-2.42	
$2p^3 2P^o *$	2.15	-1.17	-2.87	
$3s 4p$	-5.35	-8.67	-9.37	
$3s 2p$	-5.70	-9.02	-9.72	
$3p 4S^o$	-6.98	-10.30		
$3p 2D^o$	-7.02			
$3p 2P^o$	-7.14			
$3s' 2D$	-7.37			
$4s 4p$	-7.87			
Ionization	-9.56			

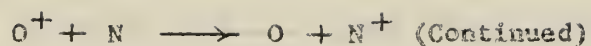


OI/OII	Ground	$2p^3 2D^o *$	$2p^3 2P^o *$
Ground	0.019	3.34	5.04
$2p^4 1D *$	-1.948	1.37	3.07
$2p^4 1S *$	-4.170	-0.85	0.85
$3s 5S^o$	-9.125	-5.81	-4.11
$3s 3S^o$	-9.500	-6.18	-4.48
$3p 5P$	-10.719	-7.40	-5.70
$3p 3P$	-10.967	-7.65	-5.95
$4s 5S^o$	-11.824	-8.50	-6.80
$3s' 1D^o$	-12.706	-9.39	-7.69
$4d 5D^o$	-12.731	-9.41	-7.71
$4d 3D^o$	-12.736	-9.42	-7.72
$5p 3P$	-12.857	-9.54	-7.84
$6s 5S^o$	-12.998	-9.68	-7.98
Ionization	-13.595	-10.28	-8.58



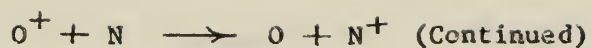
Primary ion in ground state

OI/NII	Ground	$2p^2 \ ^1D^*$	$2p^2 \ ^1S^*$	$2p^3 \ ^5S^o$	$2p^3 \ ^3D^o$	$2p^3 \ ^3P^o$	$2p^3 \ ^1D^o$
Ground	-0.93	-2.83	-4.98	-6.78	-12.36	-14.47	-18.80
$2p^4 \ ^1D^*$	-2.90	-4.80	-6.95	-8.75	-14.33	-16.44	
$2p^4 \ ^1S^*$	-5.12	-7.02	-9.17	-10.97	-16.55		
$3s \ ^5S^o$	-10.07	-11.97	-14.12	-15.92			
$3s \ ^3S^o$	-10.45	-12.35	-14.50				
$3p \ ^5P$	-11.67	-13.57					
$3p \ ^3P$	-11.92	-13.82					
$4s \ ^5S^o$	-12.77	-14.37					
$3s' \ ^1D^o$	-13.66	-15.56					
$4d \ ^5D^o$	-13.68						
$4d \ ^3D^o$	-13.69						
$5p \ ^3P$	-13.81						
$6s \ ^5S^o$	-13.95						
Ionization	-14.54						



Primary ion in  $2p^3 \ ^2D^\circ$  metastable state

OI/III	Ground	$2p^2 \ ^1D^*$	$2p^2 \ ^1S^*$	$2p^3 \ ^5S^\circ$	$2p^3 \ ^3D^\circ$	$2p^3 \ ^3P^\circ$	$2p^3 \ ^1D^\circ$
Ground	2.39	0.49	-1.66	-3.46	-9.04	-11.15	-15.58
$2p^4 \ ^1D^*$	0.42	-1.48	-3.63	-5.43	-11.01	-13.12	
$2p^4 \ ^1S^*$	-1.80	-3.70	-5.85	-7.65	-13.23		
$3s \ ^5S^\circ$	-6.75	-8.65	-10.80	-12.60			
$3s \ ^3S^\circ$	-7.13	-9.03	-11.18				
$3p \ ^5P$	-8.35	-10.25					
$3p \ ^3P$	-8.60	-10.50					
$4s \ ^5S^\circ$	-9.45	-11.05					
$3s' \ ^1D^\circ$	-10.34	-12.24					
$4d \ ^5D^\circ$	-10.36						
$4d \ ^3D^\circ$	-10.37						
$5p \ ^3P$	-10.49						
$6s \ ^5S^\circ$	-10.63						
Ionization	-11.22						



Primary ion in  $2p^3 2p^0$  metastable state

OI/NII	Ground	$2p^2 1D^*$	$2p^2 1S^*$	$2p^3 5S^0$	$2p^3 3D^0$	$2p^3 3P^0$	$2p^3 1D^0$
Ground	4.09	2.19	0.04	-1.76	-7.34	-9.45	-13.78
$2p^4 1D^*$	2.12	0.22	1.93	-3.73	-9.31	-11.42	
$2p^4 1S^*$	-0.10	-2.00	4.15	-5.95	-11.53		
$3s 5S^0$	-5.05	-6.95	9.10	-10.90			
$3s 3S^0$	-5.43	-7.33	9.48				
$3p 5P$	-6.65	-8.55					
$3p 3P$	-6.90	-8.80					
$4s 5S^0$	-7.75	-9.35					
$3s' 1D^0$	-8.64	-10.54					
$4d 5D^0$	-8.66						
$4d 3D^0$	-8.67						
$5p 3P$	-8.79						
$6s 5S^0$	-8.93						
Ionization	-9.52						

## APPENDIX C

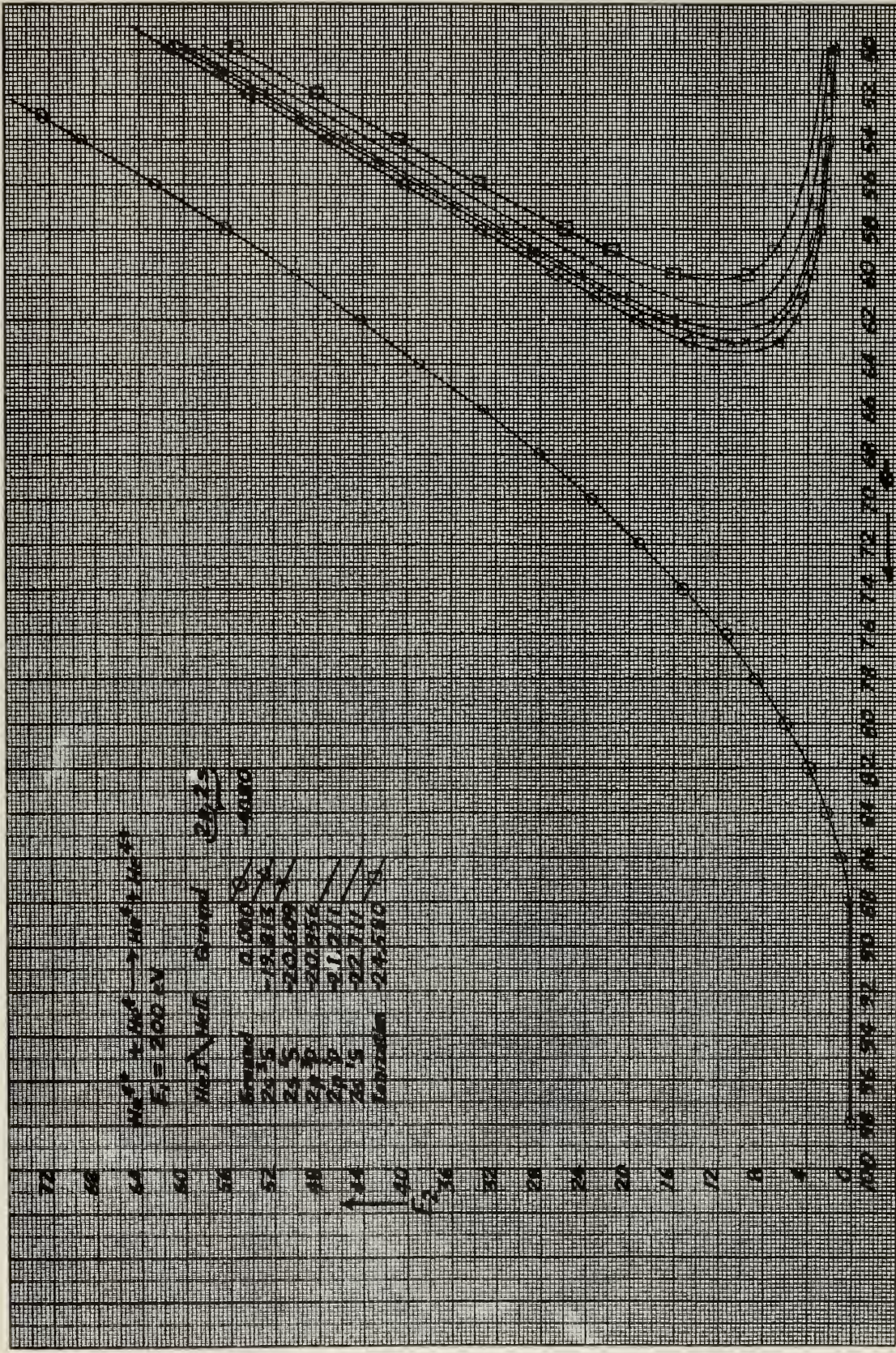
### CURVES RELATING THE ANGLE OF EMISSION OF THE SECONDARY ION TO ITS ENERGY FOR REACTIONS OF INERT GASES

The notation used in the legend of these graphs is the same as that used in appendix A. Also, as in appendix A, the AI and BII in the legend refer to the final atom and the secondary ion respectively. The initial atom and primary ion are in the ground state. All the atom excitation transitions which give rise to a  $\Delta E$  which is less in absolute value than that of the atom excitation transition with the largest absolute value of  $\Delta E$  which is plotted on the particle graph are listed in the legend.



$He^{+} + He^{+} \rightarrow He^{+} + He^{+}$   
 $E_i = 200 \text{ eV}$

$He^{+} / He^{+}$  ground  $2p, 2s$   
 Extended  
 $2s, 2p$   $0.000$   
 $2s, 2p$   $-19.813$   
 $2s, 2p$   $-20.609$   
 $2p, 2p$   $-20.956$   
 $2p, 2p$   $-21.211$   
 $2s, 2s$   $-22.711$   
 Extended  $-24.580$





72

68

64

60

56

52

48

44

40

36

E<sub>2</sub>

32

28

24

20

16

12

8

4

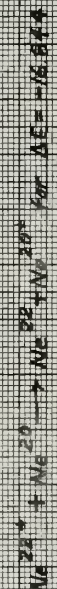
0

100 98 96 94 92 90 88 86 84 82 80 78 76 74 72 70 68 66 64 62 60 58 56 54 52 50

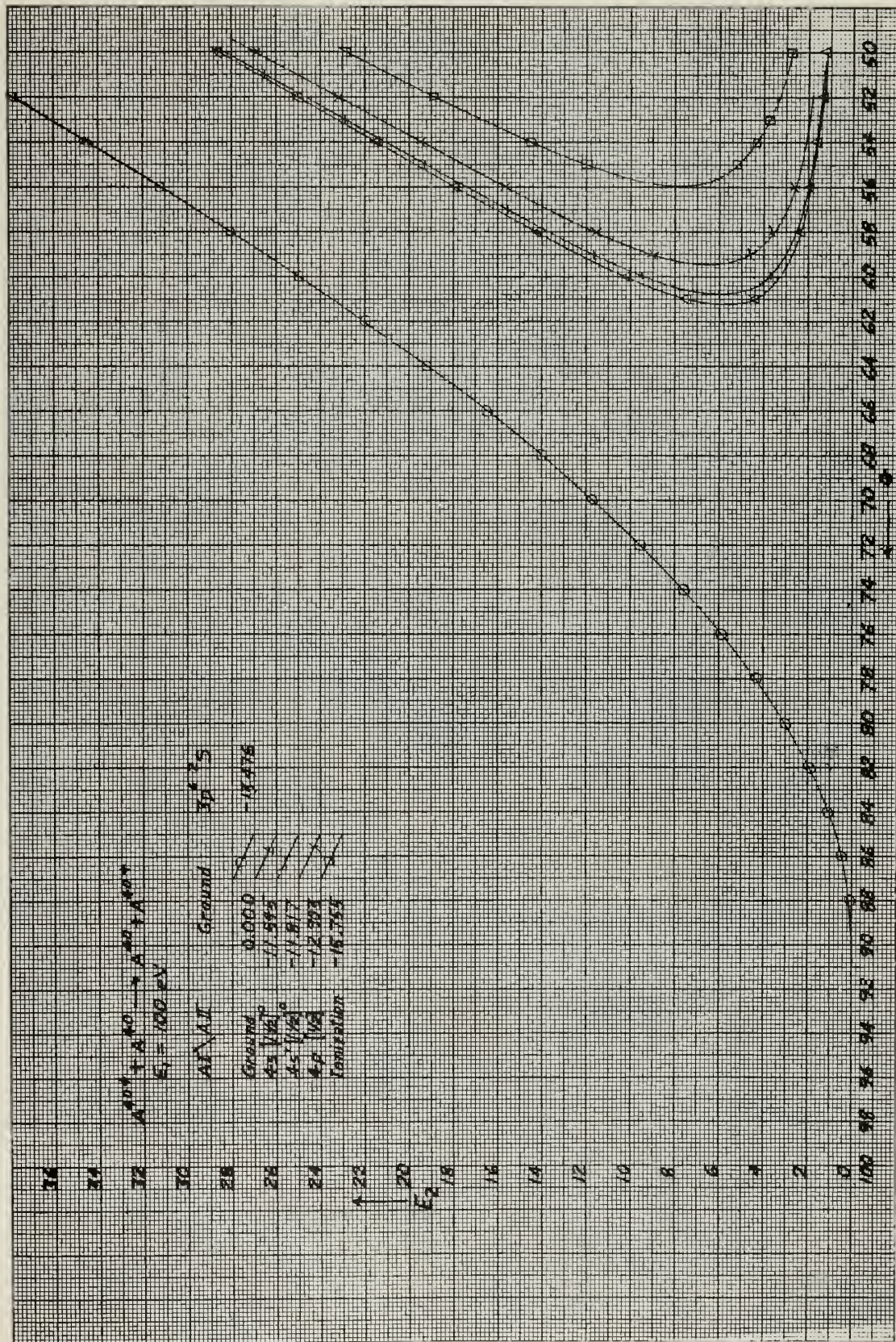


Ne I Ne II	Ground	2p <sup>5</sup> 3s
Ground	0.000	-26.503
3s $1/2$	-16.615	
3s $3/2$	-16.711	
3s $5/2$	-16.844	
3p $1/2$	-18.377	
Ionization	-21.553	

★ The dashed line represents each of the reactions









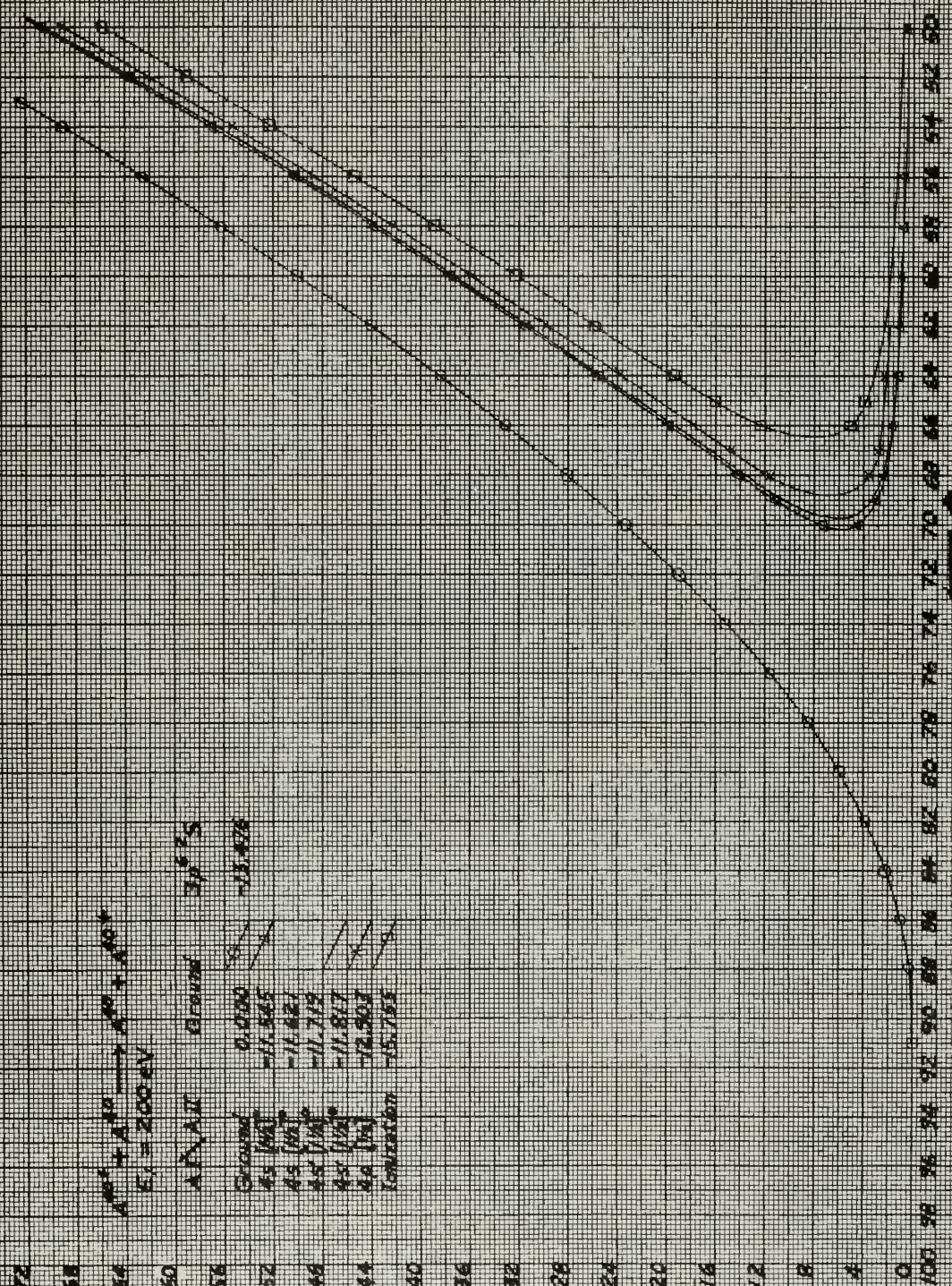
72  
68  
64  
60  
56  
52  
48  
44  
40  
36  
32  
28  
24  
20  
16  
12  
8  
4  
0

$10^4 + 10 \rightarrow 10^4 + 10^4$   
 $E_1 = 200 \text{ eV}$

APXII	Ground	$3p^2S$
Ground	0.000	-13.476
$4s [M]$	-11.545	
$4s [M]$	-11.427	
$4s [M]$	-11.712	
$4s [M]$	-11.817	
$4s [M]$	-12.503	
Ionization	-15.755	

$E_2$

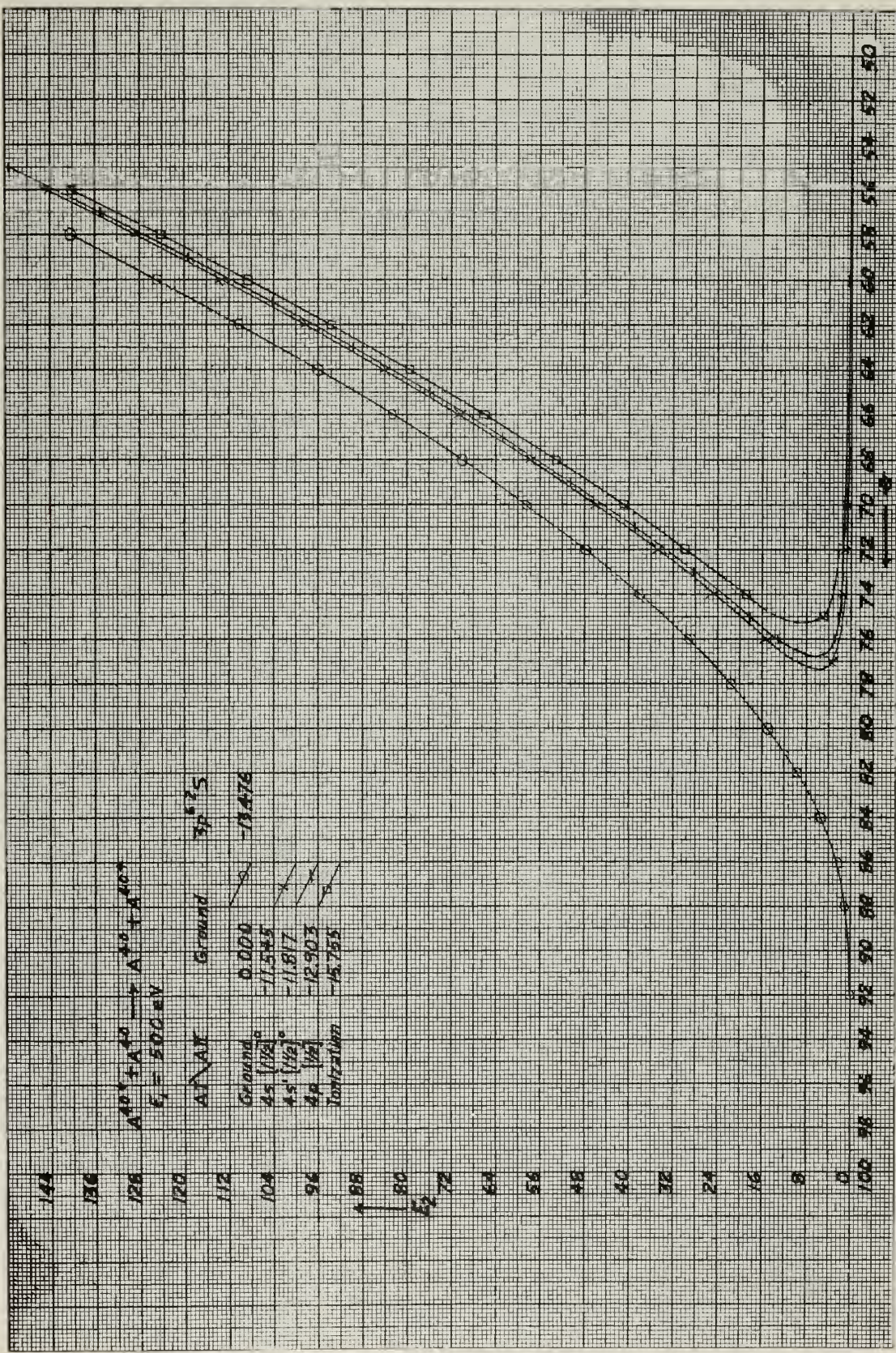
100 98 96 94 92 90 88 86 84 82 80 78 76 74 72 70 68 66 64 62 60 58 56 54 52 50





$A^{10} + A^{10} \rightarrow A^{20} + A^{10}$   
 $E_i = 500 \text{ eV}$

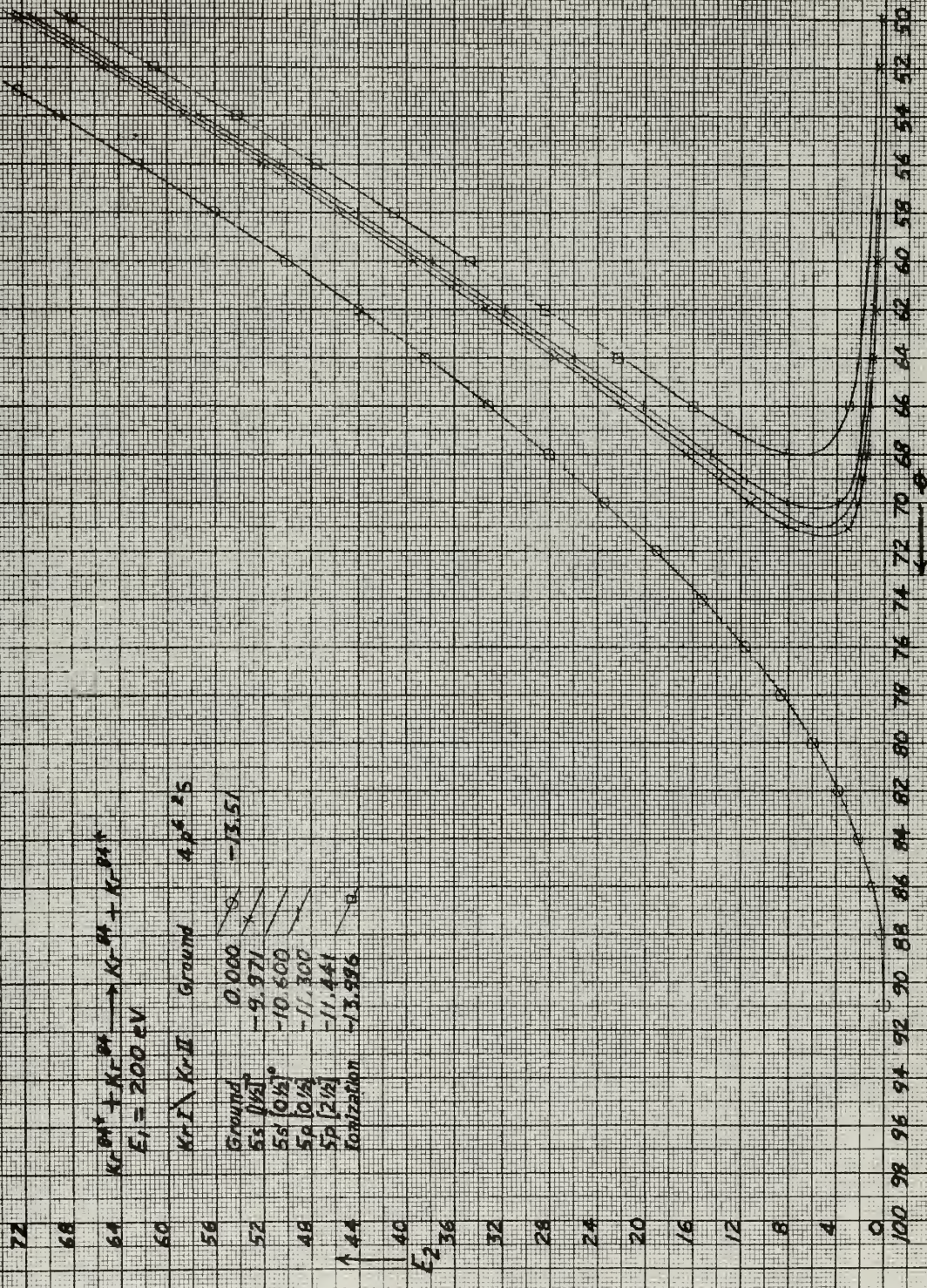
$A^{10} + A^{10}$	Ground	$3p^2 2s$
Ground	0.000	-13.476
$4s \left[ \frac{1}{2} \right]_0$	-11.545	
$4s' \left[ \frac{1}{2} \right]_0$	-11.817	
$4p \left[ \frac{1}{2} \right]$	-12.903	
Ionization	-15.755	



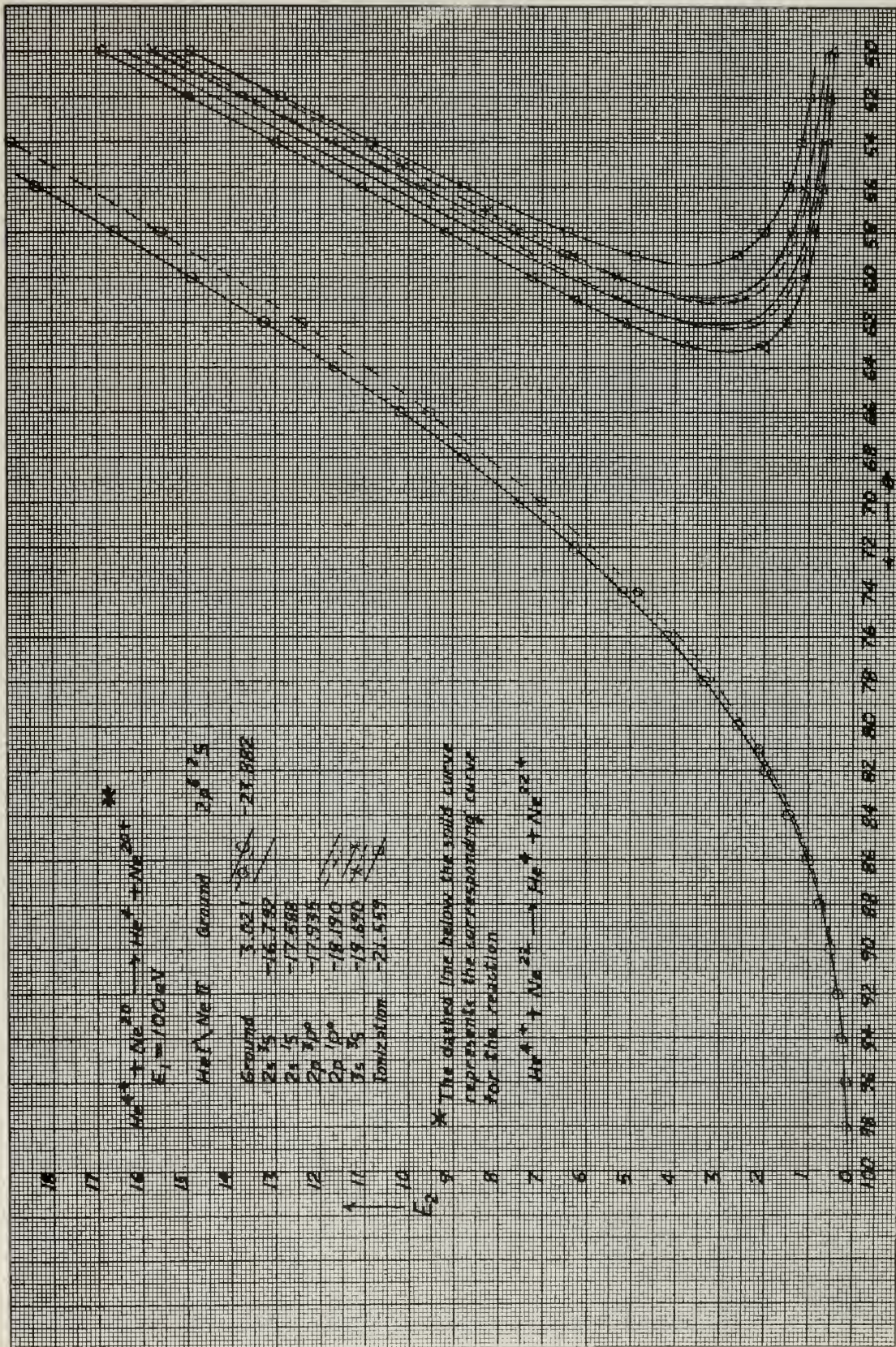


$Kr^{84} + Kr^{84} \rightarrow Kr^{84} + Kr^{84}$   
 $E_1 = 200 \text{ eV}$

$Kr I \backslash Kr II$	Ground	$4p^5 2s$
Ground	0.000	-13.51
$5s [1/2]$	-9.971	
$5s [0 1/2]$	-10.600	
$5p [0 1/2]$	-11.300	
$5p [2 1/2]$	-11.441	
Ionization	-13.996	



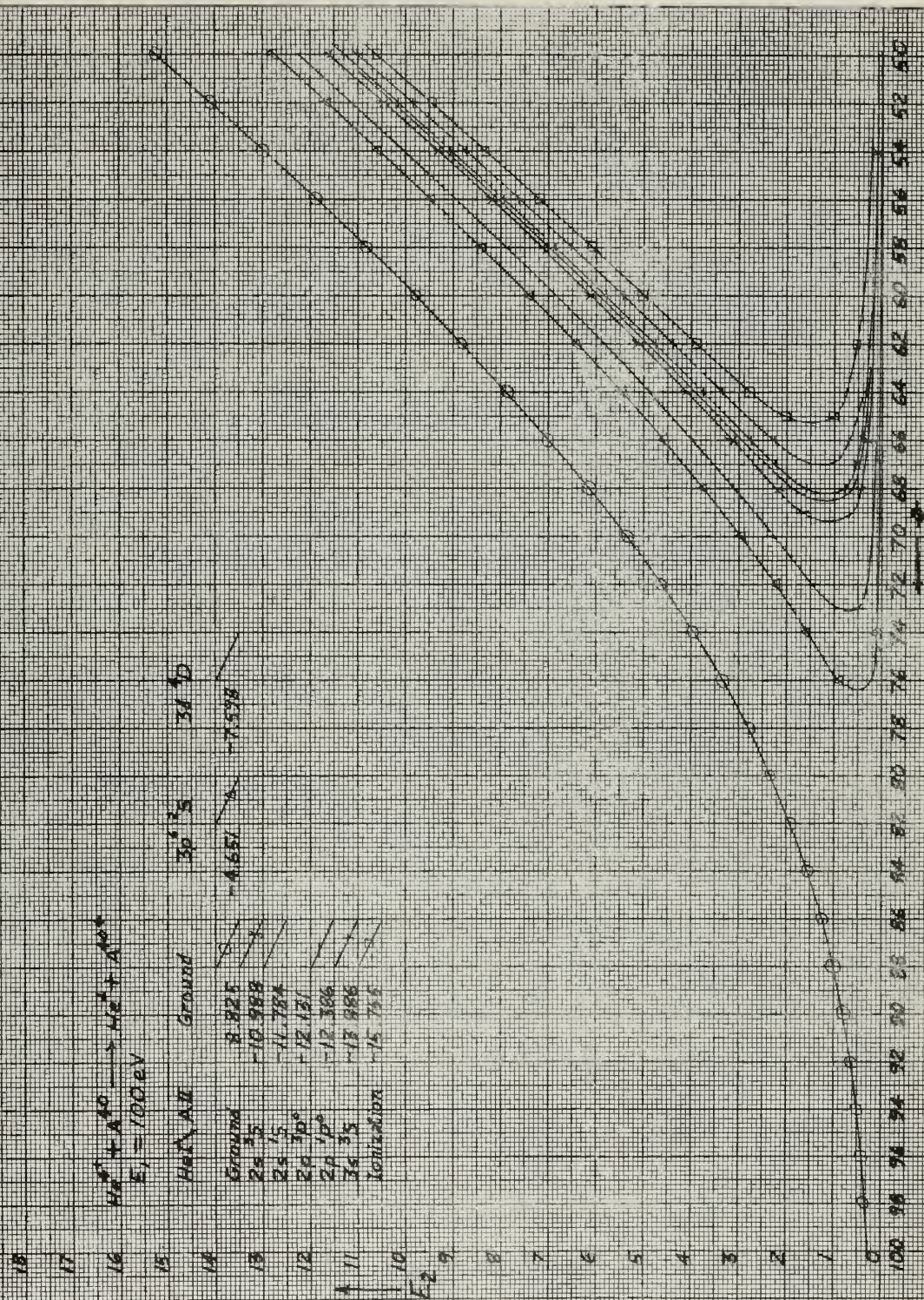






$H\alpha^+ + A^{10} \rightarrow H\alpha^+ + A^{10+}$   
 $E_i = 100 \text{ eV}$

$H\alpha^+ A^{10}$	Ground	$3p^1 \text{ } ^2S$	$3d^1 \text{ } ^2D$
Ground	8.825	-8.651	-7.598
$2s^1 \text{ } ^2S$	-10.988		
$2s^1 \text{ } ^1S$	-11.784		
$2p^1 \text{ } ^2P^o$	-12.131		
$2p^1 \text{ } ^1P^o$	-12.386		
$3s^1 \text{ } ^2S$	-13.888		
Ionization	-15.755		





18

17



He I \ Kr II

Ground

Ground	10.584
2s 3s	-9.229
2s 3s	-10.025
2p 3p	-10.372
2p 3p	-10.627
3s 3s	-12.127
Ionization	-13.996

He I \ Kr II

Ground

5s 4p

5s 4p

5s 4p

5s 4p

5s 4p

5s 4p

5s 4p

5s 4p

5s 4p

5s 4p

5s 4p

5s 4p

5s 4p

5s 4p

5s 4p

5s 4p

5s 4p

5s 4p

5s 4p

5s 4p

5s 4p

5s 4p

5s 4p

5s 4p

18

17

16

15

14

13

12

11

10

9

8

7

6

5

4

3

2

1

0

100

98

96

94

92

90

18

17

16

15

14

13

12

11

10

9

8

7

6

5

4

3

2

1

0

100

98

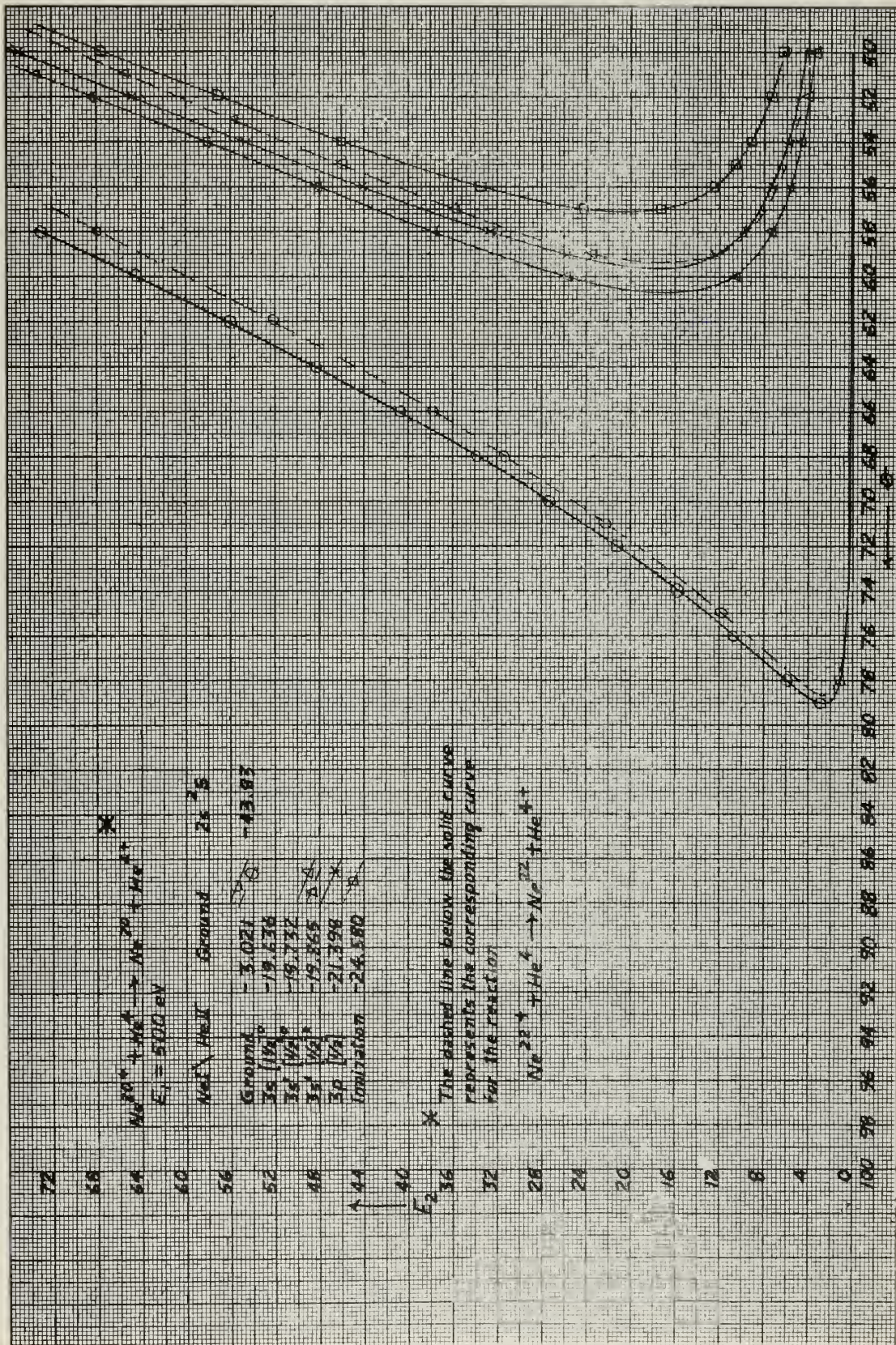
96

94

92

90







36

34

32

30

28

26

24

22

20

18

16

14

12

10

8

6

4

2

0

100

98

96

94

34

32

30

28

26

24

22

20

18

16

14

12

10

8

6

4

2

0

100

98

96

94

92

32

30

28

26

24

22

20

18

16

14

12

10

8

6

4

2

0

100

98

96

94

92

90

30

28

26

24

22

20

18

16

14

12

10

8

6

4

2

0

100

98

96

94

92

90

28

26

24

22

20

18

16

14

12

10

8

6

4

2

0

100

98

96

94

92

90

88

86

26

24

22

20

18

16

14

12

10

8

6

4

2

0

100

98

96

94

92

90

88

86

84

82

80

78

76

74

72

70

68

24

22

20

18

16

14

12

10

8

6

4

2

0

100

98

96

94

92

90

88

86

84

82

80

78

76

74

72

70

68

66

64

22

20

18

16

14

12

10

8

6

4

2

0

100

98

96

94

92

90

88

86

84

82

80

78

76

74

72

70

68

66

64

62

60

20

18

16

14

12

10

8

6

4

2

0

100

98

96

94

92

90

88

86

84

82

80

78

76

74

72

70

68

66

64

62

60

18

16

14

12

10

8

6

4

2

0

100

98

96

94

92

90

88

86

84

82

80

78

76

74

72

70

68

66

64

62

60

16

14

12

10

8

6

4

2

0

100

98

96

94

92

90

88

86

84

82

80

78

76

74

72

70

68

66

64

62

60

14

12

10

8

6

4

2

0

100

98

96

94

92

90

88

86

84

82

80

78

76

74

72

70

68

66

64

62

60

12

10

8

6

4

2

0

100

98

96

94

92

90

88

86

84

82

80

78

76

74

72

70

68

66

64

62

60

10

8

6

4

2

0

100

98

96

94

92

90

88

86

84

82

80

78

76

74

72

70

68

66

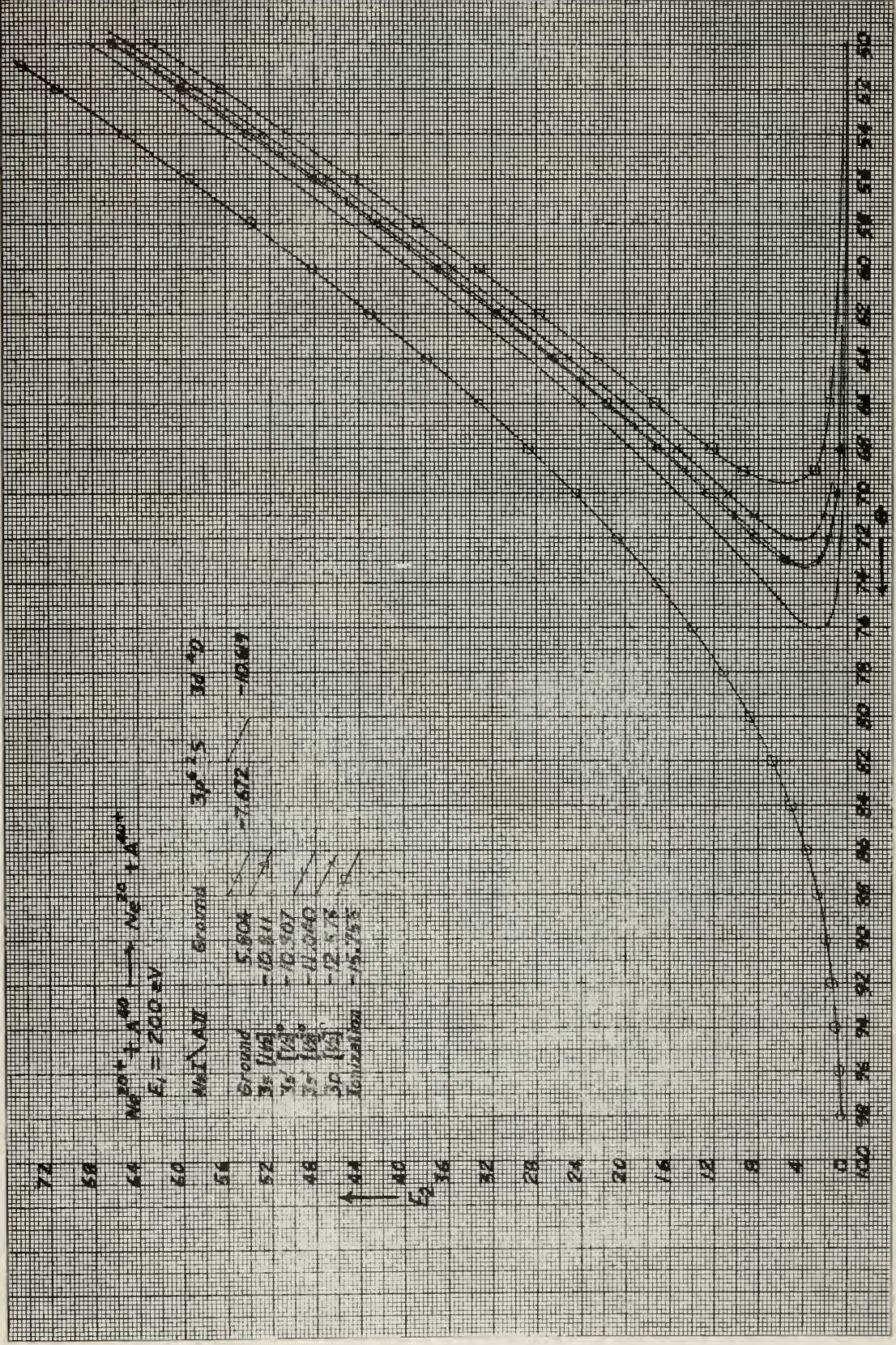
64

62

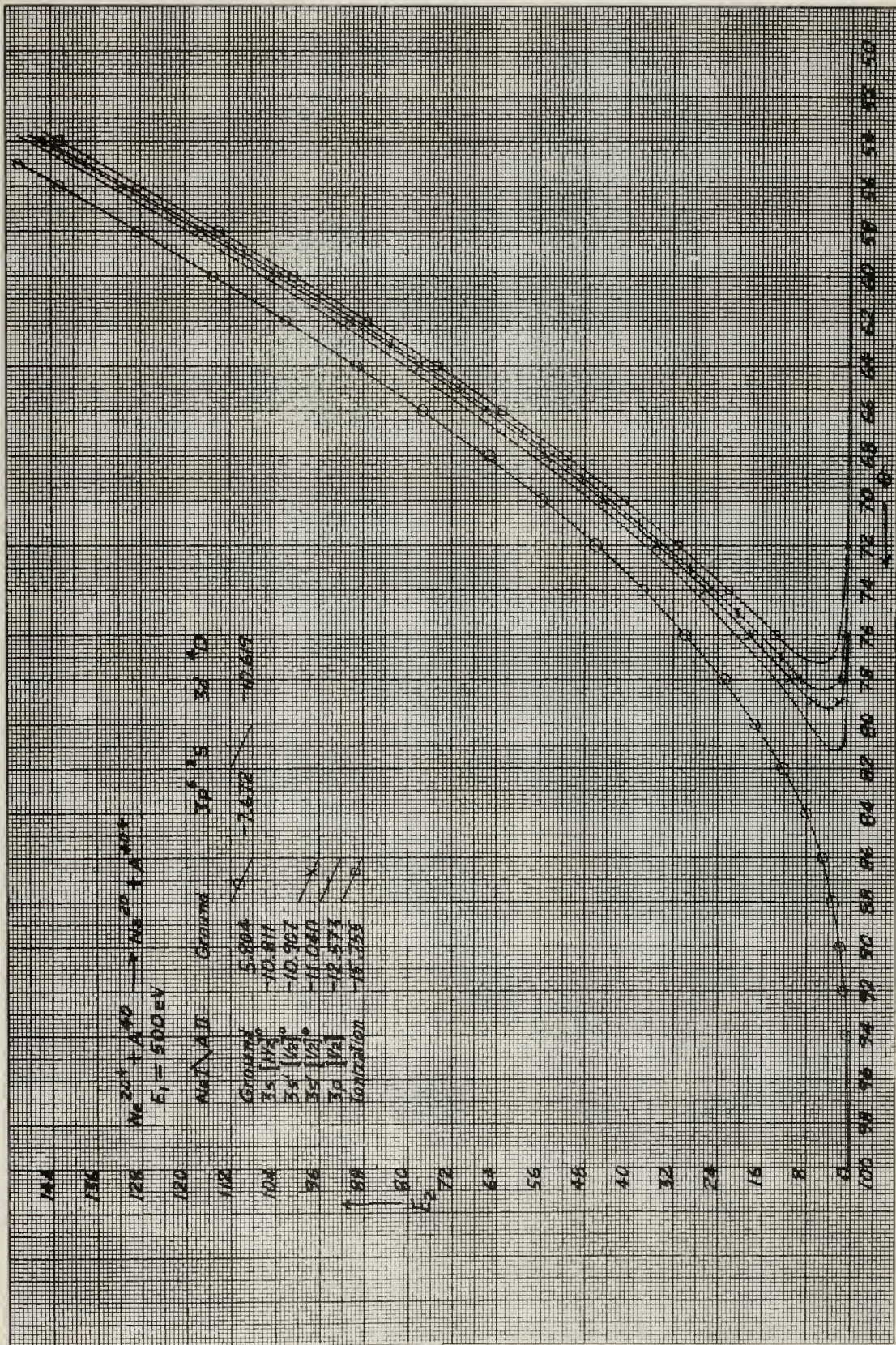
60

8











72  
68  
64  
60  
56  
52  
48  
44  
40  
36  
32  
28  
24  
20  
16  
12  
8  
4  
0

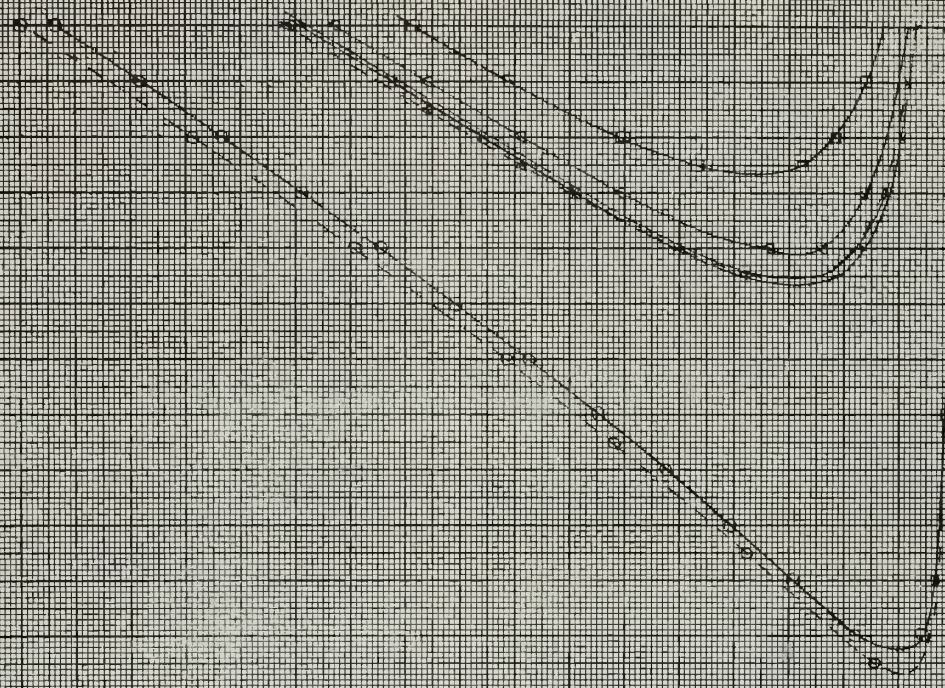
$A^{20} + Ne^{20} \rightarrow A^{40} + Ne^{20}^*$   
 $E_i = 200 \text{ eV}$

$A^{20} \backslash Ne^{20}$	Ground	$20^{+2}S$
Ground	-5.804	-32.70
$2s [Ne]$	-17.349	
$4s [Ne]$	-17.621	
$4p [Ne]$	-18.707	
Ionization	-21.959	

\* The dashed line above the solid curve represents the corresponding curve for the reaction

$A^{20} + Ne^{20} \rightarrow A^{40} + Ne^{20}^*$

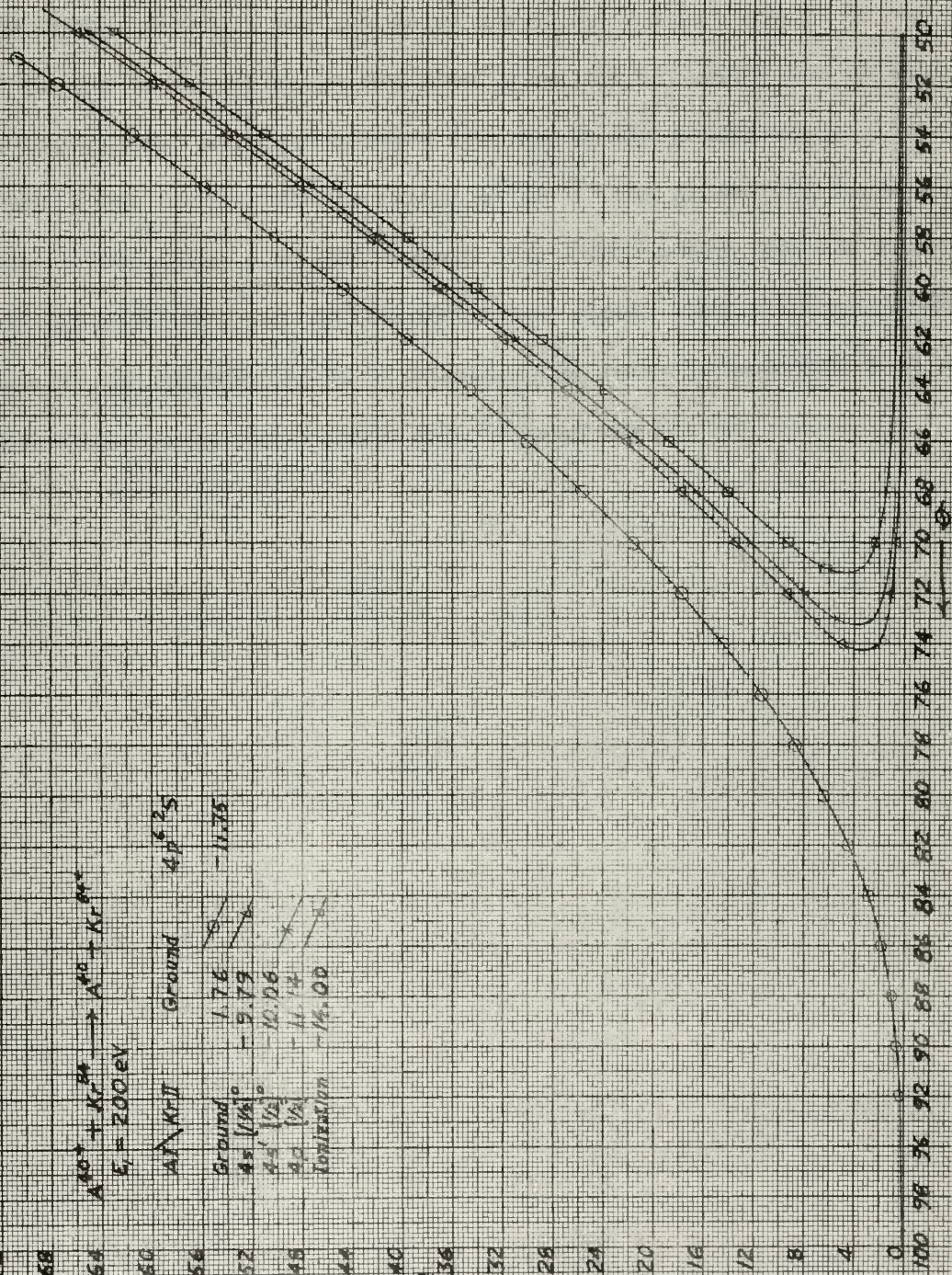
600 98 96 94 92 90 88 86 84 82 80 78 76 74 72 70 68 66 64 62 60 58 56 54 52 50







AI/Kr II	Ground	$4p^6 2s$
Ground	1.76	-11.75
$4s \ 1/2$	-9.79	
$4s' \ 1/2$	-10.06	
$4p \ 1/2$	-11.12	
Ionization	-12.00	





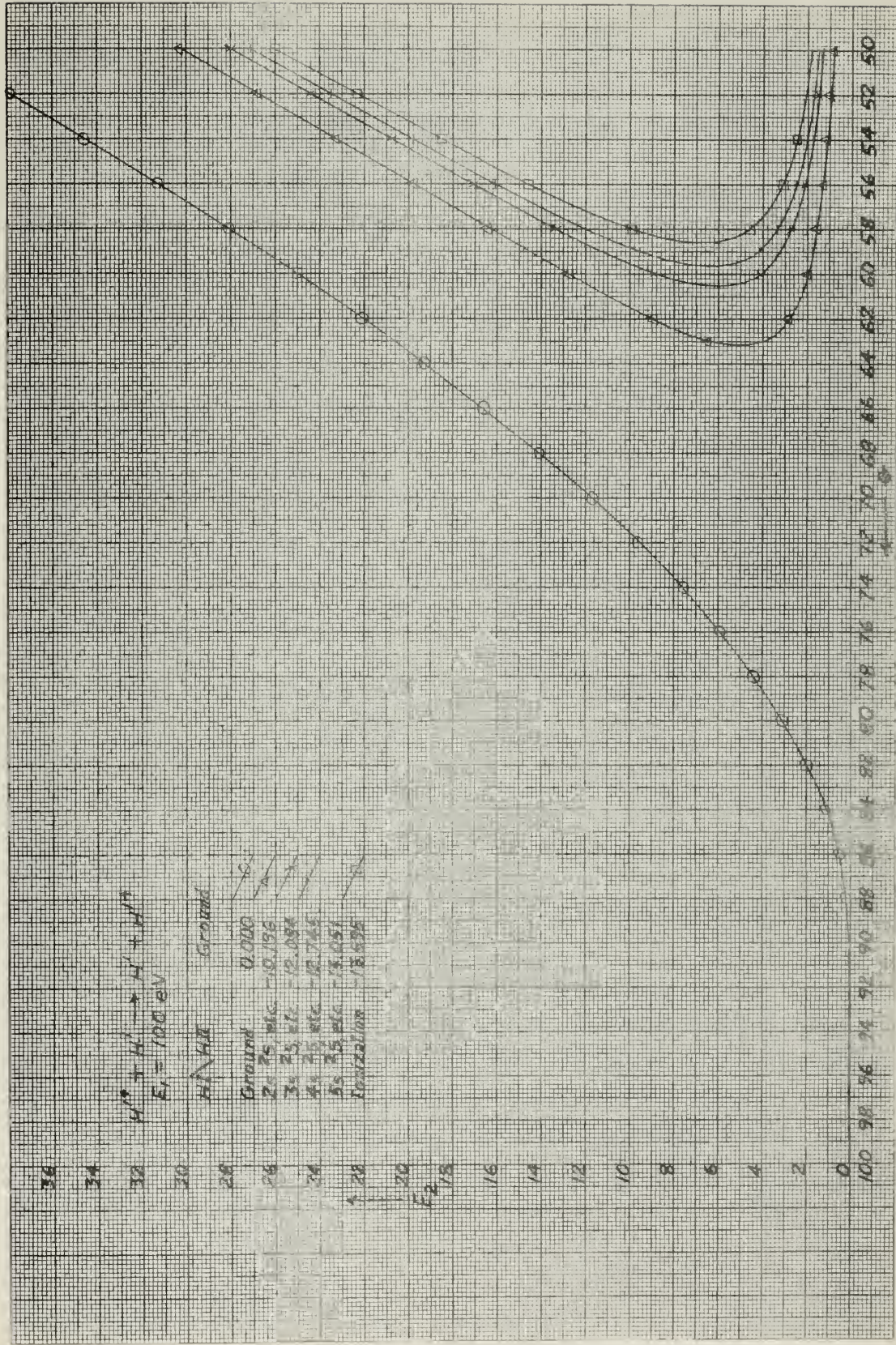
## APPENDIX D

### CURVES RELATING THE ANGLE OF EMISSION OF THE SECONDARY ION TO ITS ENERGY FOR REACTIONS OF HYDROGEN, NITROGEN, AND OXYGEN

The notation used in the legend of these graphs is the same as that used in appendix B. For graphs in which the initial ion is  $H^+$  the AI and BII in the legend refer to the final atom and secondary ion respectively, and the initial atom and primary ion are in the ground state. For graphs in which the initial ion is either  $N^+$  or  $O^+$  the AI and BII in the legend refer to the final atom and primary ion respectively, and the initial atom and secondary ion are in the ground state. Not all transitions are shown in the legend, so it is necessary to refer to appendix B to find other transitions which might fall between the curves plotted.

$H^+ + H^+ \rightarrow H^+ + H^+$   
 $E_i = 100 \text{ eV}$

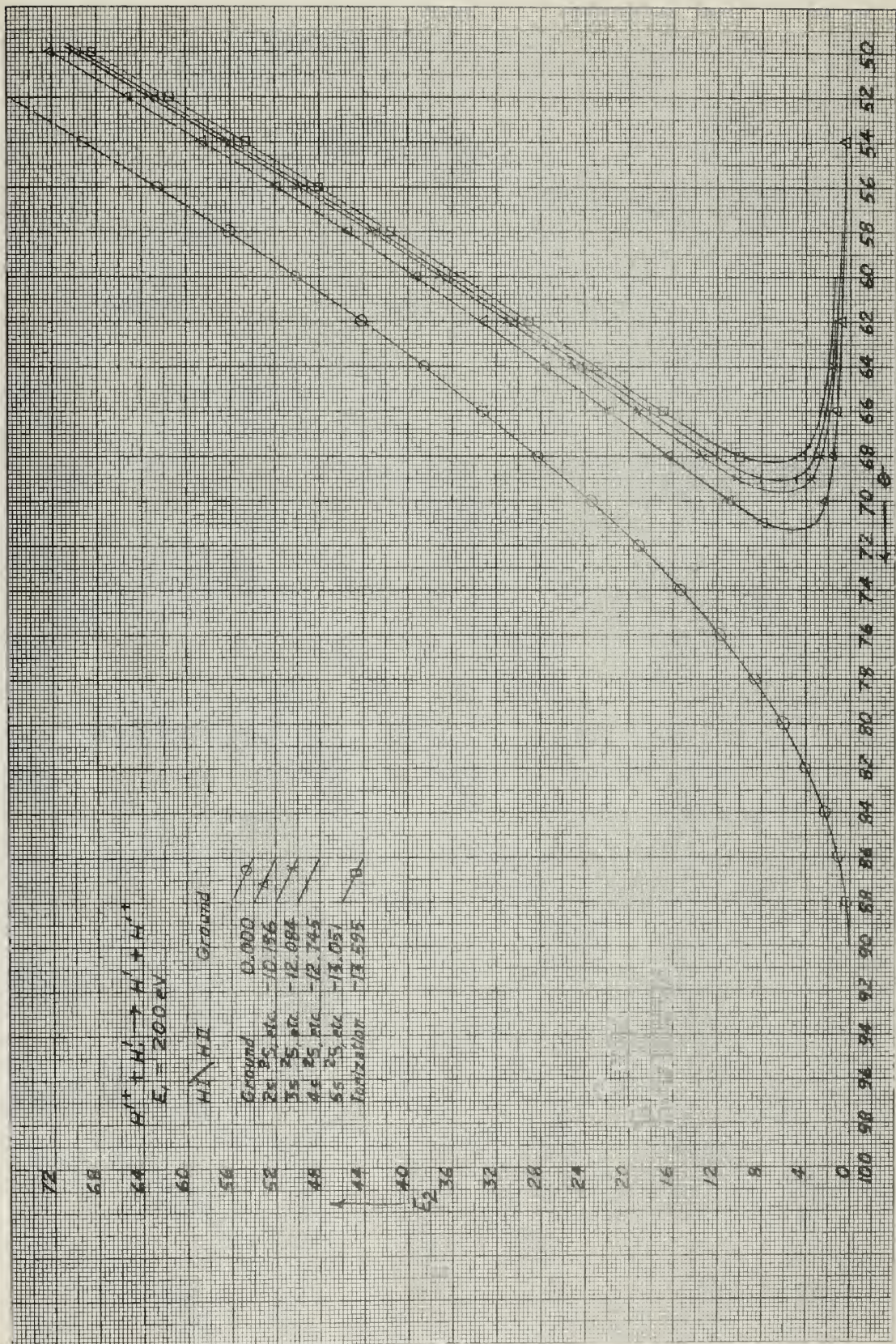
$H^+ H^+$	Ground	$\rho_i$
Ground	0.000	0
2, 25 etc	-10.198	1
3, 23 etc	-12.094	2
4, 25 etc	-12.745	3
5, 25 etc	-13.051	4
Ionization	-13.605	5



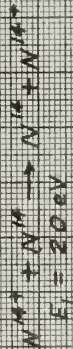


$H'' + H' \rightarrow H' + H''$   
 $E_i = 200 \text{ eV}$

$H' \setminus H''$	Ground	
Ground	0.000	0
25, etc.	-10.196	1
35, etc.	-12.084	2
45, etc.	-12.745	3
55, etc.	-13.051	4
Ionization	-13.595	5

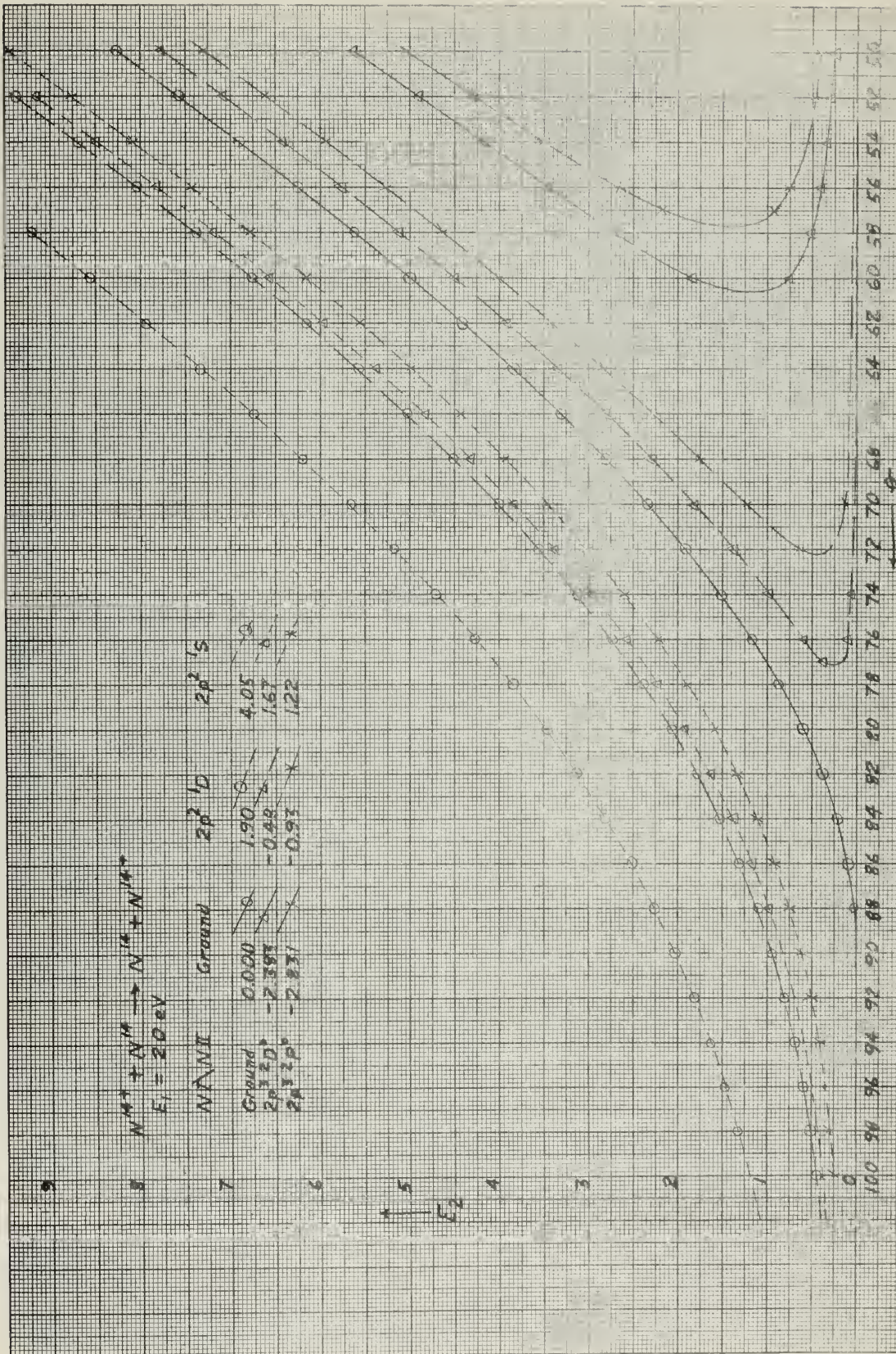






$N^{14} N^{14}$	Ground	$2p^2 \text{ } ^1D$	$2p^2 \text{ } ^3S$
Ground	0.000	1.90	4.05
$2p^3 \text{ } ^3D$	-2.393	-0.48	1.67
$2p^4 \text{ } ^3P$	-2.831	-0.93	1.22

$F_2$





36



$N^{14+}$	$N^{14+}$	Ground	$2p^2 \text{ } ^1D$	$2p^2 \text{ } ^3S$
Ground	Ground	0.00	1.90	4.05
$2p^2 \text{ } ^1D$	$2p^2 \text{ } ^1D$	-2.88	-0.48	1.67
$2p^2 \text{ } ^3S$	$2p^2 \text{ } ^3S$	-2.83	-0.93	1.22
$3s \text{ } ^2P$	$3s \text{ } ^2P$	-10.68	-8.78	-6.63
$3p \text{ } ^4S$	$3p \text{ } ^4S$	-11.99	-10.09	-7.94
$3s^2 \text{ } ^1D$	$3s^2 \text{ } ^1D$	-12.35	-10.45	-8.30
$4s \text{ } ^4P$	$4s \text{ } ^4P$	-12.85	-10.95	-8.80
Ionization	Ionization	-14.54	-12.64	-10.49

$E_2$

18

16

14

12

10

8

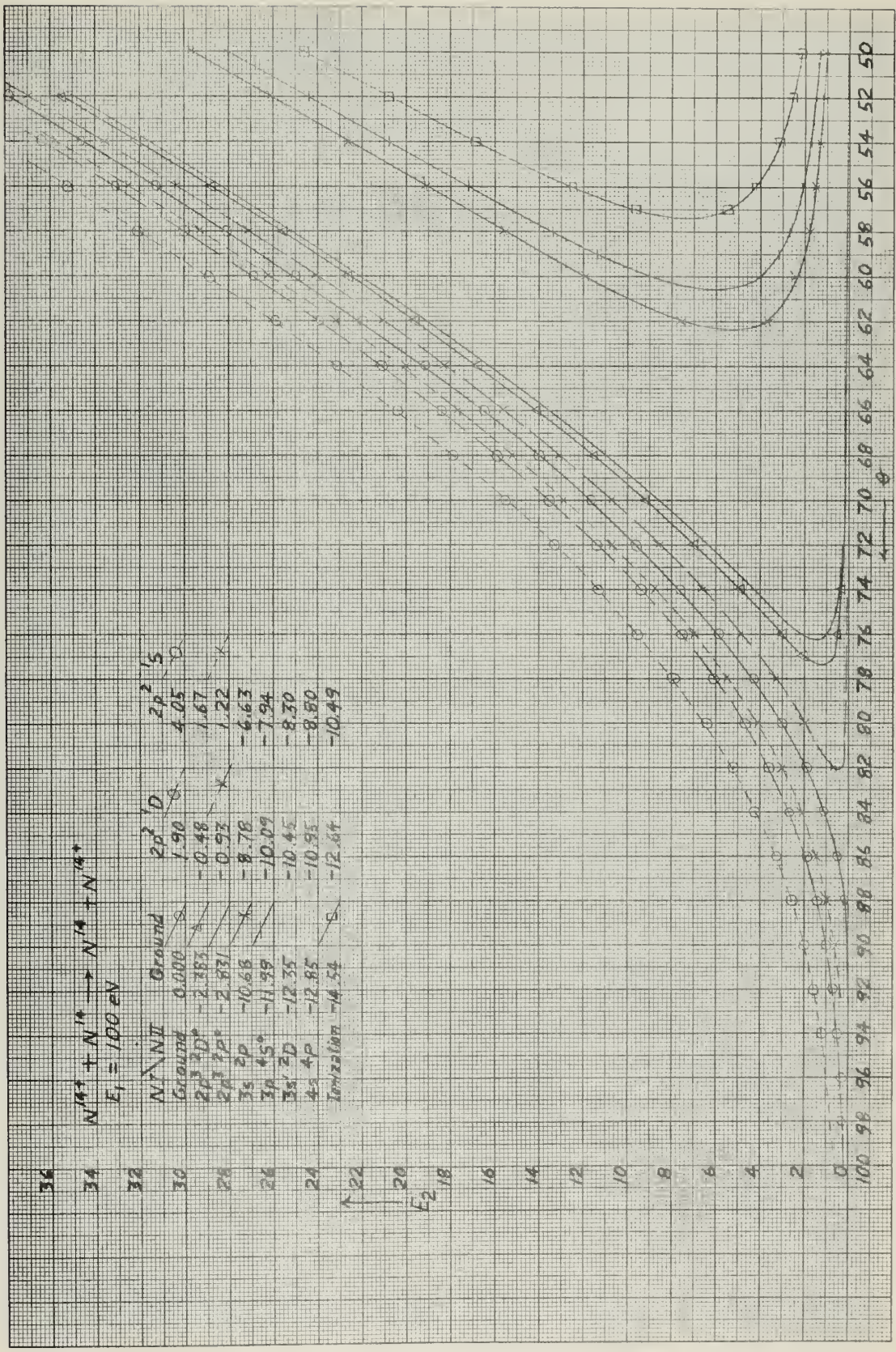
6

4

2

0

100 98 96 94 92 90 88 86 84 82 80 78 76 74 72 70 68 66 64 62 60 58 56 54 52 50

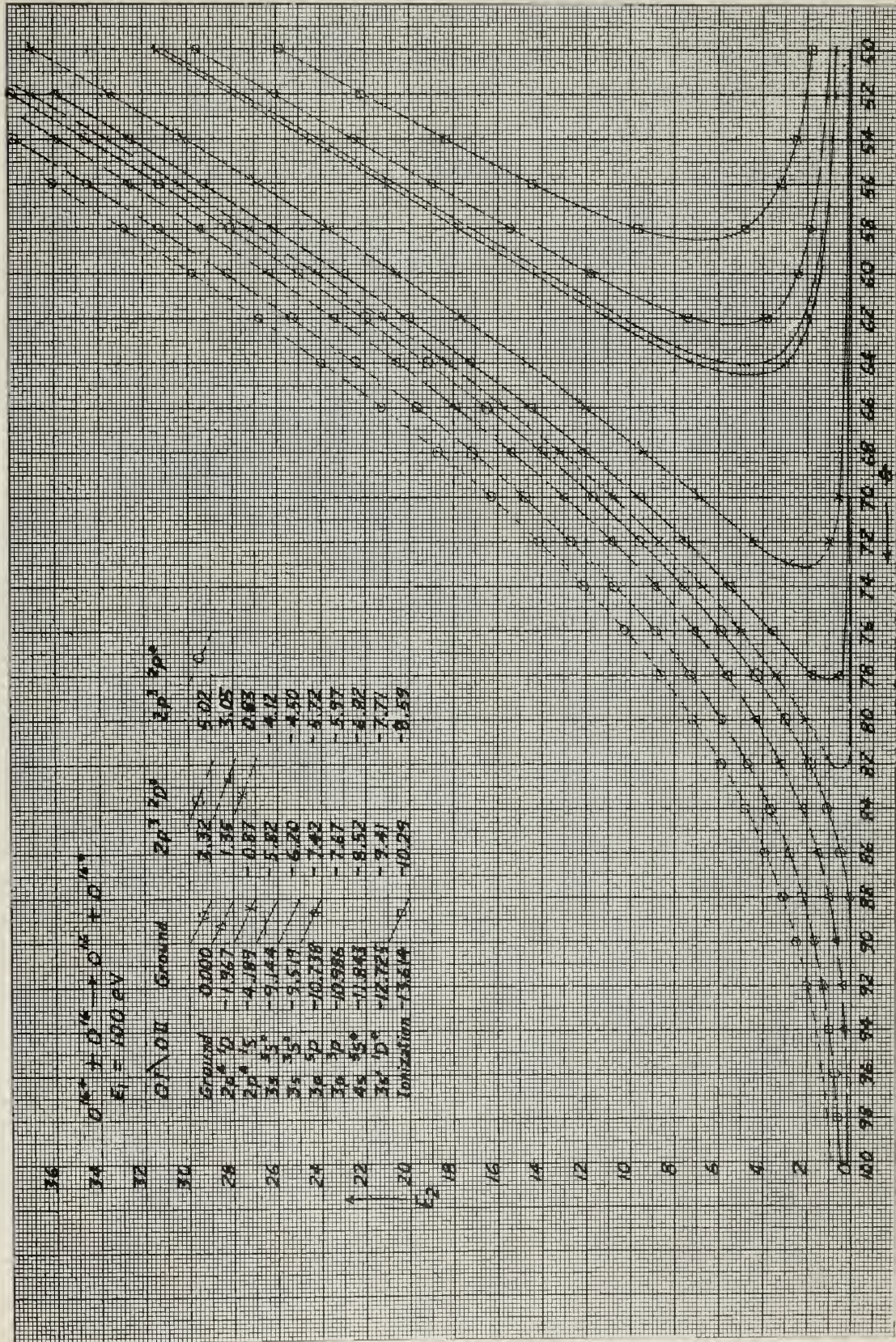




$$0.16 + 0.16 + 0.16 + 0.16$$

$$E_1 = 100 \text{ eV}$$

$0.16$	Ground	$2p^3 2D$	$2p^3 2P^o$
Ground	0.000	3.32	5.02
$2p^3 2D$	-1.967	1.35	3.05
$2p^3 2P^o$	-4.189	-0.87	0.83
$3s^3 3S^o$	-9.144	-5.82	-4.12
$3s^3 3P^o$	-5.519	-6.20	-4.50
$3p^3 3P$	-10.738	-7.42	-5.72
$3p^3 3D$	-10.986	-7.67	-5.97
$4s^3 4S^o$	-17.843	-8.52	-6.82
$3d^3 3D^o$	-12.725	-9.41	-7.71
Ionization	-13.614	-10.29	-8.59

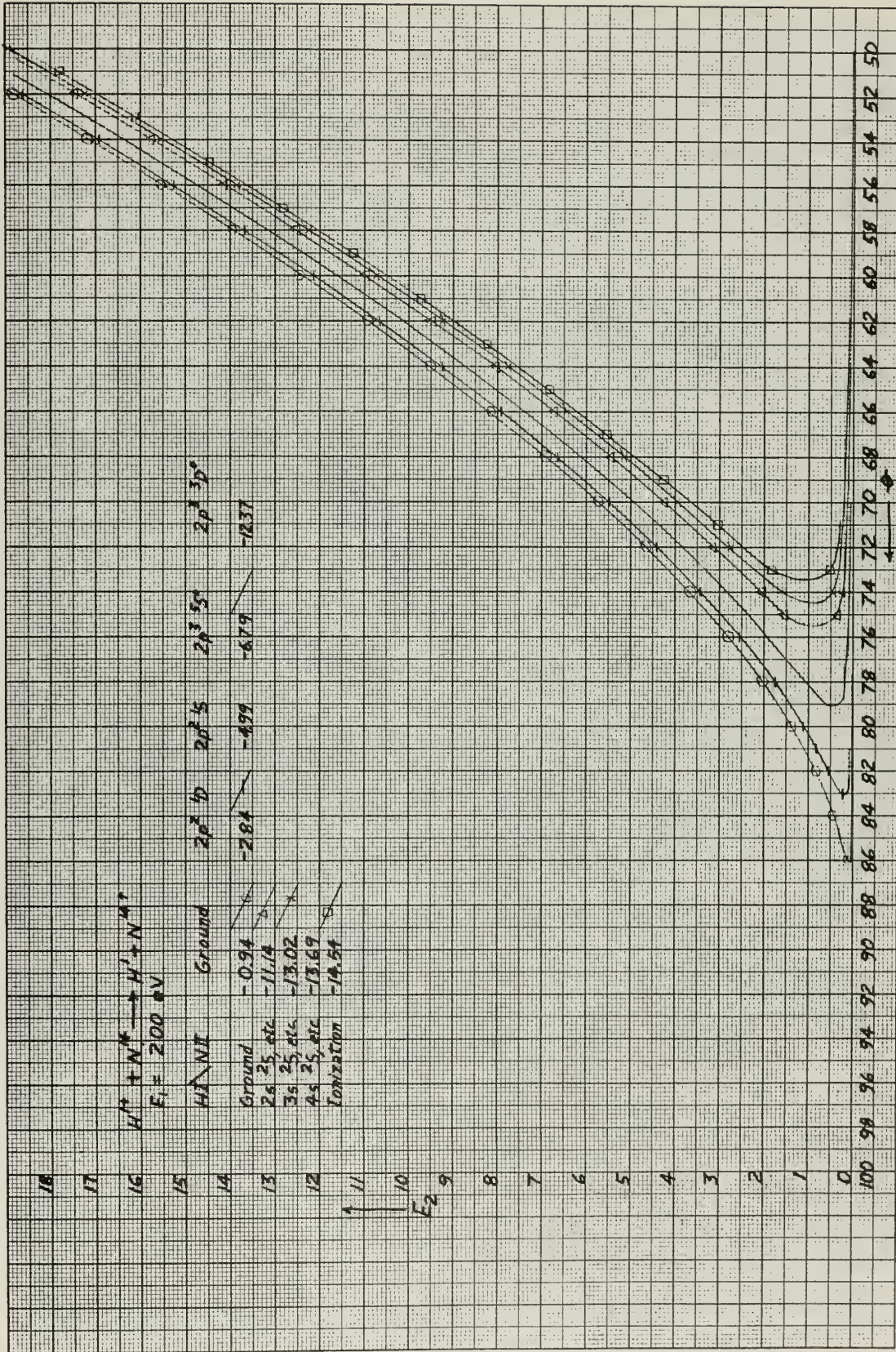




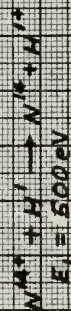


$E_1 = 200 \text{ eV}$

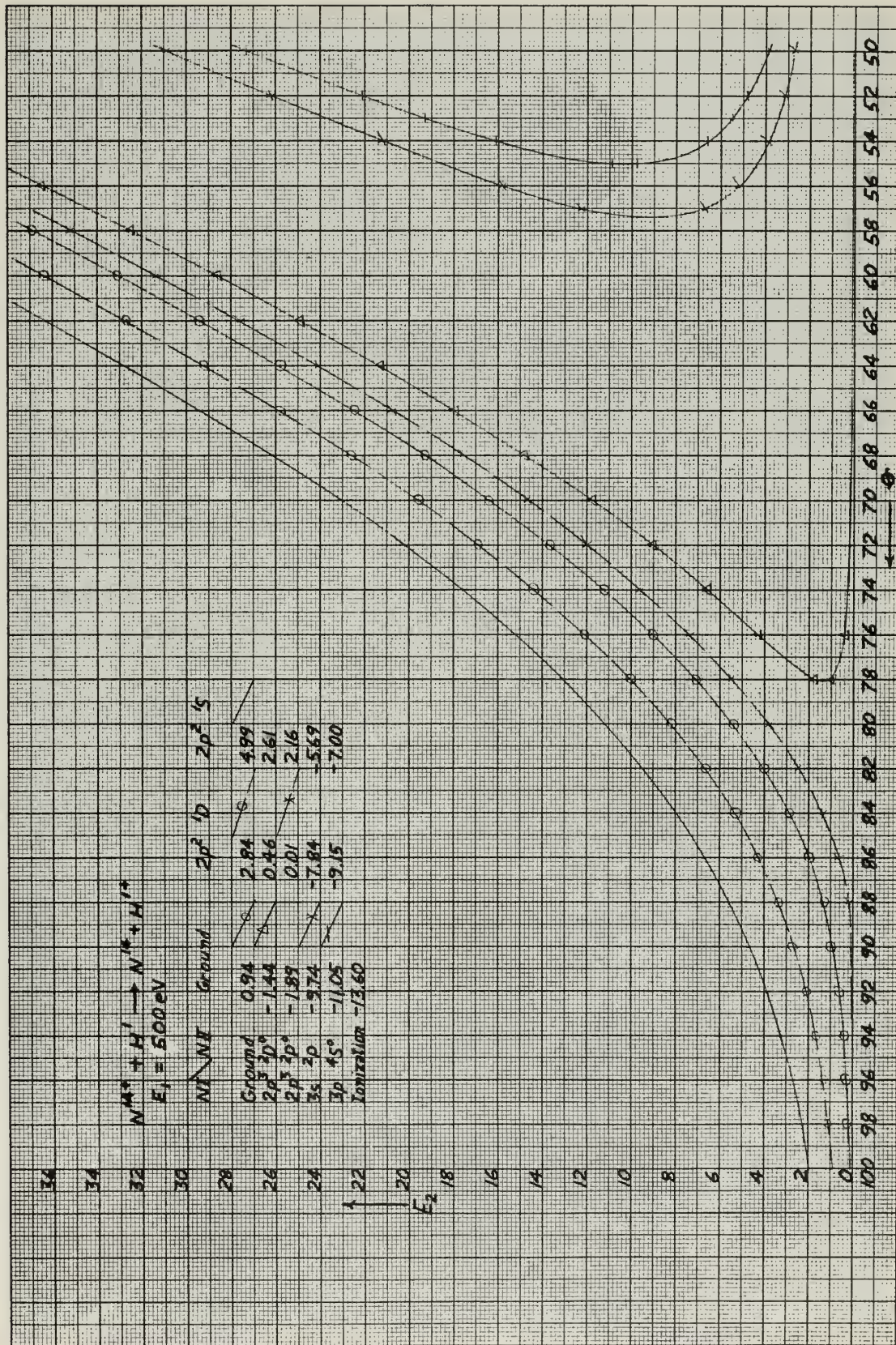
HI/NI	Ground	$2p^2 \text{ } ^3\text{P}$	$2p^2 \text{ } ^3\text{S}$	$2p^2 \text{ } ^3\text{D}$
Ground	-0.94	-2.84	-4.99	-12.37
$2s \text{ } ^2\text{S}$ , etc.	-11.14			
$3s \text{ } ^2\text{S}$ , etc.	-13.02			
$4s \text{ } ^2\text{S}$ , etc.	-13.69			
Ionization	-14.54			







Ni	NI	Ground	2p <sup>3</sup> 'D	2p <sup>2</sup> 'S
Ground	0.94		2.84	4.99
2p <sup>3</sup> 2D°	-1.44		0.46	2.61
2p <sup>3</sup> 2p°	-1.89		0.01	2.16
3s 2p	-9.74		-7.84	-5.69
3p 4s°	-11.05		-9.15	-7.00
Ionization -13.60				

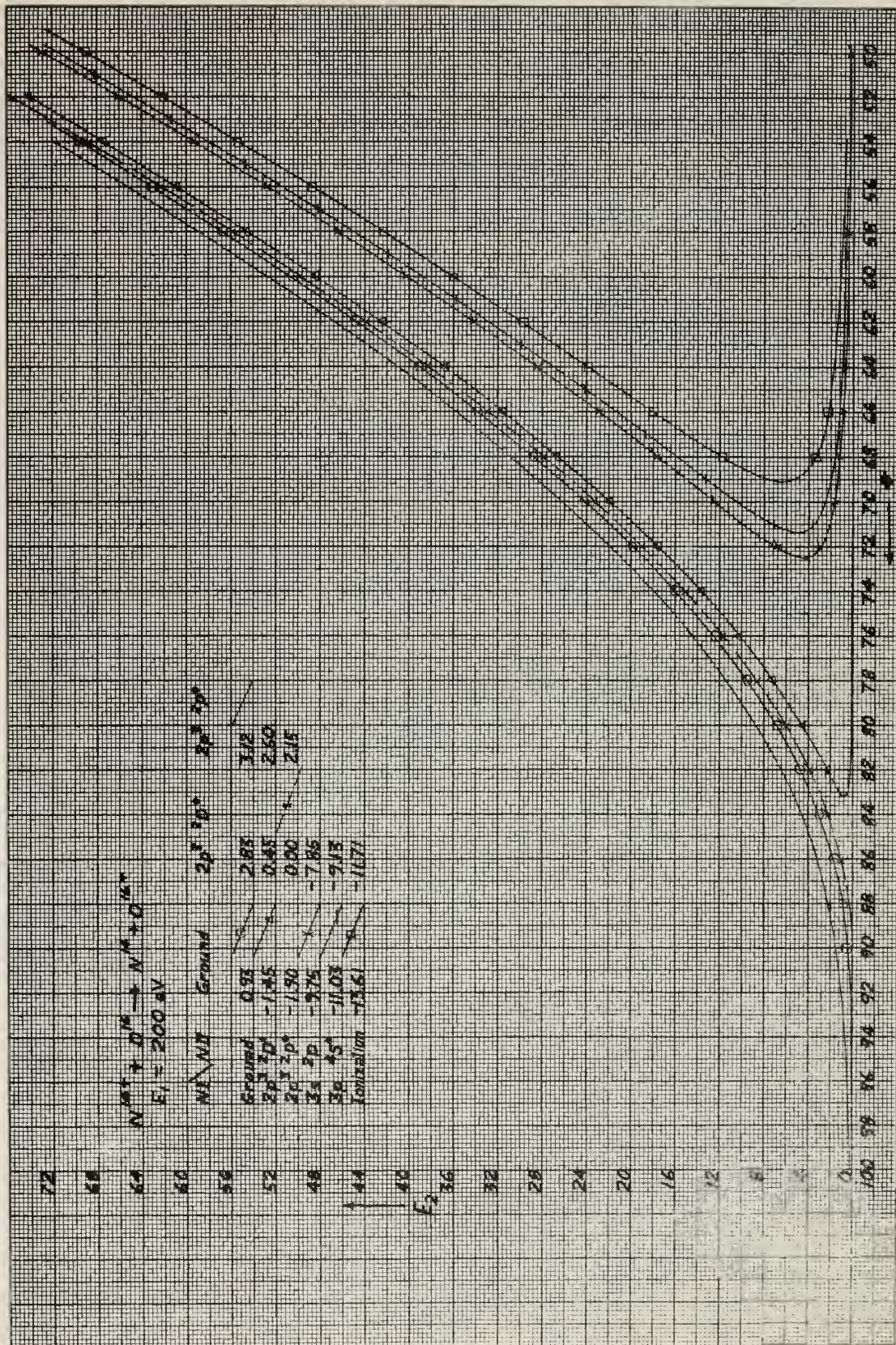




$$N^{10^5} + 0^{10^5} \rightarrow N^{10^5} + 0^{10^5}$$

$$E_1 = 200 \text{ eV}$$

NI	NI	Ground	$2p^3 2p^3$	$2p^3 2p^3$
Ground	0.93		2.85	3.12
$2p^3 2p^3$	-1.45		0.45	2.60
$2p^3 2p^3$	-1.90		0.00	2.15
$3s 2p$	-3.75		-7.85	
$3s 4s$	-11.03		-9.13	
Ionization	-13.61		-16.71	



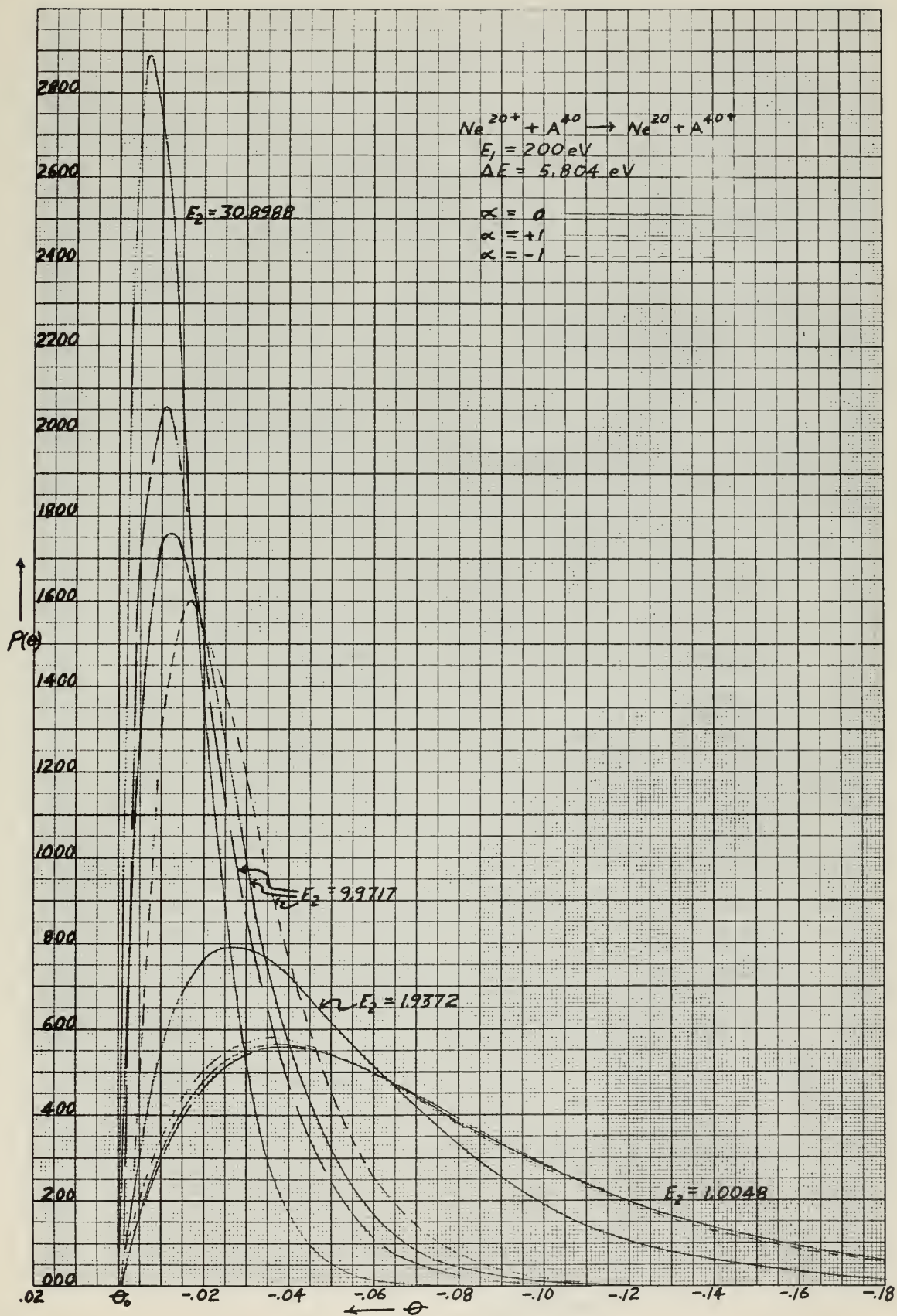


## APPENDIX E

### THE ANGULAR DISTRIBUTION OF SECONDARY IONS OF A FIXED ENERGY DUE TO THE DISTRIBUTION OF SPEEDS OF THE INITIAL ATOM

The ordinate  $\theta_0$  is the angle that the secondary ion would be emitted at with the fixed energy ( $E_2$ ) of the curve under consideration if  $E_0$  were equal to zero. This is the angle found in appendix C or D for a given energy  $E_2$ . The decimal value of the ordinates to the left of  $\theta_0$  are to be added to this value of  $\theta_0$ . The decimal value of ordinates to the right of  $\theta_0$  are to be subtracted from this value of  $\theta_0$ .

The abscissa represents the relative density of secondary ions.





4000



$E_1 = 200 \text{ eV}$

3600

$Q = -5.204 \text{ eV}$

$m = 0$

$m = 1$

3200

2800

Prod.

2400

1600

1200

800

400

000

$E_2 = 36.70613$

$E_2 = 35.85705$

$E_2 = 9.5711$

.12

.10

.08

.06

.04

.02

0

-.02

$\theta$



thesS5717

Kinematics of atomic charge-transfer col



3 2768 002 01160 3

DUDLEY KNOX LIBRARY